UNIVERSITÀ DEGLI STUDI DI PAVIA
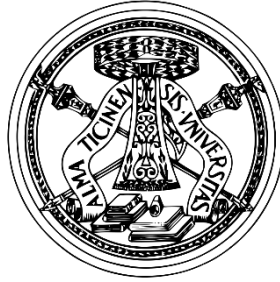
Dipartimento di Scienze Clinico-Chirurgiche, Diagnostiche e Pediatriche

Dottorato di ricerca in Medicina Sperimentale – Ciclo XXII

Coordinatore: Ch.mo Prof. Carlo Maurizio Montecucco

"Mesenchymal stromal cells on bioscaffold for liver bioengineering"

Tesi di:

Dott.ssa Stefania Croce

Relatore:

Prof. Lorenzo Cobianchi

Correlatori:

Dott.ssa M. Antonietta Avanzini

Dott. Andrea Peloso

aa 2018/2019

CONTENTS:

ABBREVIATIONS:

2D: bi-dimensional

3D: three-dimensional

AA: Acetic acid

AA1T-D: antitrypsin deficiency

ALB: albumin

AFP: alpha fetoprotein

AP: alkaline phosphatase

ATMP: Advanced Therapy Medicinal Products

BALs: bioartificial livers

BSA: Bovine serum albumin

bFGF: basic fibroblast growth factor

BM: bone marrow

Ca^{2+}: Calcium ions

$Ca(OH)_2$: Calcium hydroxide

CAM: chorioallantoic membrane

CBD: common bile duct

CHAPS: 3-[(3-cholamidopropyl) dimethylammonio]-1-propanesulfonate

CK: cytokeratin

cPD: cumulative population doublings

COMMD1: copper metabolism domain containing 1

c-Myc: c-myc oncogene

CYP450: Cytochrome P450

CYP7A1: Cytochrome P450 subunit 7A1

DAPI: 4,6-diamidino-2-phenylindole

hDLM: decellularized human liver matrix

dH_2O: distilled water

DNA: DeoxyriboNucleic Acid

DNasi: Deoxyribonuclease

DWJS: decellularized Wharton's jelly scaffolds

ECM: extracellular matrix

EDC: 1-ethyl-3-(3-dimethylaminopropyl)-carbodiimide

EDTA: ethylenediaminetetraacetic acid

EFG: Epidermal Growth Factor

EGTA: ethylene glycol tetra-acetic acid

ELISA: enzyme-linked immunosorbent assay

ESCs: embryonic stem cells

EtOH: ethanol hydroxide

EA.hy926: human endothelial hybrid cell line

FACS: fluorescence-activated cell sorting

FCS: fetal calf serum

FITC: Fluorescein isothiocyanate

GADPH: glyceraldehyde 3 phosphate dehydrogenase

GAGs: glycosaminoglycans

GDA: glutaraldehyde

HA: hepatic artery

HepG2: liver hepatocellular cells

HGF: hepatocyte growth factor

H&E: hematoxylin and eosin

HLCs: hepatocyte like cells

HNF: Hepatocyte Nuclear Factor

IGF-1: insuline-like growth factor-1

iHPCs: immortalized fetal hepatic progenitor cells

iPSCs: induced pluripotent stem cells

IVC: inferior vena cava

Klf4: Kruppel-like factor 4

LX-2: human hepatic stellate cell line-2

MNCs: Mononuclear cells

MTT: 1-(4,5-Dimethylthiazol-2-yl)-3,5-diphenylformazan

pMSCs: porcine mesenchymal stromal cells

Mg^{2+}: Magnesium ions

NaCl: Sodium chloride

NaOH: sodium hydroxide

Na_2S: sodium sulphide

NH_4OH: ammonium hydroxide

NHS: N-hydroxysuccinimide

OBE: organ bioengineering

Oct4: octamer-binding transcription factor 4

OD: Optical density

PAA: Paracetic acid

PAS: Periodic acid–Schiff

PBS: Phosphate-buffered saline

PCL: polycaprolactone

PE: phycoerythrin

PEG: polyethylene glycol

PFA: Paraformaldehyde

pLgr5: p-Leucine-rich repeat-containing G protein coupled receptor 5

PLLA: poli-L-lactic acid

PV: portal vein

RGD: tripeptide Arginine-Glycine-Aspartate

RM: Regenerative medicine

RNA: RiboNucleic Acid

RNasi: Ribonuclease

SA: Sulfuric acid

SCB: Sodium Cacodylate Buffer

SDC: Sodium deoxycholate

SDS: Sodium dodecyl sulphate

SEM: Scanning electron microscopy

Sk-Hep-1: human hepatic adenocarcinoma cells

Sox2: SRY-box 2

SPARC: Secreted Protein Acidic and Rich in Cysteine

SVC: superior vena cava

UVA: Ultraviolet A

UVECs: umbelical vein endothelial cells.

VEGF: Vascular endothelial growth factor

SUMMARY

Liver transplantation represent the only successful treatment for chronic end-stage liver disease as well as acute liver failure. However, the shortage of organ donors results every year in the death of many patients in the waiting list. To overcome the lack of donors it is mandatory to develop new therapeutic options.

In the last decades, organ bioengineering has been extensively explored to create transplantable and functional tissues or whole organs. The final goal of organ bio-engineering is the use of the bioengineered organs as 'replacement parts' for the human body. Moreover, the advantage of this technology is the use of autologous cells that eliminates the need for post-transplant immunosuppression.

In the present study, we decellularized pig livers and repopulated them with allogeneic porcine mesenchymal stromal cells (pMSCs) to study the interaction between pMSCs and liver specific extracellular matrix (ECM). The aim of this study was to understand if ECM can influence and/or promote pMSCs toward differentiation into hepatocytes or hepatocyte-like cells (HLCs) without specific growth factors in culture medium. Our experimental design was divided into different steps in order to define:

• the optimal liver decellularization strategy;

• the isolation, expansion and characterization of pMSCs;

• the recellularization strategy of ECM;

• the liver specific functions in pMSCs cultured on native ECM.

In our project, porcine livers were obtained by a surgical technique similar to the one used for multi-organ explant in a human cadaveric donor. Liver samples were cut and then decellularized through agitation with 0.15% SDS. The quality of the decellularization was evaluated both qualitatively and quantitatively, with histological staining (H&E and DAPI) and DNA extraction respectively.

pMSCs were isolated from the porcine bone marrow (BM) and expanded in vitro. pMSC were characterized by assessment of morphology, proliferation capacity, immunophenotype and their differentiation ability.

After characterization, pig MSCs were used for seeding the liver scaffolds with static culture method. The scaffold recellularization was evaluated at 3, 7, 14 and 21 days after seeding with H&E, DAPI, MTT assay and SEM analysis. Moreover, in order to determinate whether culture on liver ECM-scaffold could promote/address the differentiation of pMSCs towards hepatocytes, the transcriptional levels of some genes associated to different phases of the hepatic development were tested. A comparison with the expression profile was made with both porcine primary hepatocyte and pMSC.

The observations obtained so far allow us to state that:

• our decellularization protocol is effective in the removal of the cells from native liver, respecting the parameters for decellularization without damage the structure of ECM;

• porcine MSCs obtained from porcine BM have characteristic phenotypically and functionally comparable to those of their human counterparts and therefore they can be used as a model for experimental studies such as for liver ECM recellularization;

• the static seeding strategy of pMSCs on the scaffold resulted to be effective in terms of ECM cell attachment, cell proliferation and migration inside the specimen;

• the genic profile of cells seeded on ECM scaffold without any growth factors is more similar to pMSCs suggesting that the only contact with liver specific ECM is not strong enough to induce a complete differentiation in HLCs. Despite this, we observed that Cyp7a1 gene, expressed in hepatocyte but not in MSC, was present in pMSCs seeded scaffolds at each time points.

In conclusion, we can observe that our results are in accordance with data reported in literature and sustain the possibility to use decellularizated organs as biological scaffold to create functional organs. We believe that our results may provide new insights toward a better understanding of early HLCs development on ECM-scaffolds. However, a more detailed decellularization process, a better cell differentiation capacity and a more

detailed understanding of the interaction between cells and ECM could represent crucial steps in the progression of this research field.

1. INTRODUCTION

Liver dysfunction is one of the major health problems in the world characterized by high morbidity and mortality [1]. Liver transplantation is the only successful treatment for chronic end-stage liver disease as well as acute liver failure [2][3]. Shortage of organs has led to use marginal grafts as an option to increase the organ supply, however the problem of limited number of organ donors still remains unsolved [4]. To overcome the lack of donors it is mandatory to develop new therapeutic options, such as cell-based therapies that include liver cell transplantations, bioartificial livers and engineered hepatic tissues [5][6][7]. Hepatocyte transplantation has been clinically performed for more than 20 years. Primary hepatocytes were injected into liver of patient trying to restore liver activity and metabolic functions in the recipient. Although, the replacement of 2-5% of liver cells with primary hepatocytes could improve significantly liver functions, a general problem of this approach is the limited repopulation capacity of engrafted cells. Moreover, the inability to monitor graft health and frequent cases of rejection makes hepatocyte transplantation not widely adapt in clinical practice[6].

Recently, liver regenerative medicine-based strategies such as bioartificial devices (BALs) and liver on-a-chip platform have been developed in order to temporarily support the organ until transplantation. BALs could eliminate toxins accumulating in liver failure and supply liver cells supporting the organ in synthetic and regulatory functions [8]. Liver on a chip platform is an artificial model of liver structure in a microfluidic cell culture device. This miniaturized microscale chip is able to mimic the *in vivo* physiological fluid flow condition and control temporal and spatial distribution of nutrients and growth factors to cells in a model of chronic liver disease [9][10]. Until now, BALs and liver on a chip are not a permanent alternative to liver transplantation and there are no strong evidence supporting the survival benefits of patients utilizing these devices.

In the last decades, organ bioengineering (OBE) has been extensively explored to provide transplantable tissues or whole organs. Bioengineering of complex organs requires the recapitulation of macromolecules and vascular system structure. The principle of these

procedure assumes that a variety of cells can be seeded onto an appropriate surface in a specific growth and differentiation environment. These surfaces called "scaffolds" can be derived from synthetic or biological sources. Synthetic scaffolds are produced with different technique including electrospinning [11], three-dimensional (3D) bioprinting technology [12] and hydrogel-based technologies [13]. Most of these technologies are also used not only directly for transplantation purposes, but to overcome the drawbacks of in-vitro liver testing during drugs development. Biological scaffolds are obtained from discarded organs through different decellularization methods [14][15].

1.1. Regenerative medicine and cell-on-scaffold technology application to liver transplantation

Allogeneic liver transplantation is still considered the gold standard solution for end-stage organ failure like end-stage liver disease, providing better quality of life as well as cost effectiveness; however, shortage of donor organs has resulted in extending transplantation waiting lists. In details, data from USA report more than 15000 patient added in waiting list and needing a liver transplantation with only around 6000 liver transplants performed yearly. This results in an increasing mismatch between liver donors and recipients. In the last decades, regenerative medicine (RM) and OBE has shown a great potential to overcome the limit of organs availability and to allow transplant without immunosuppression. In general, RM and OBE share the same goal trying to replace or regenerate human tissue or organ in order to restore or re-establish its native function [16][17].

Regenerative medicine paradigm consists of three important factors: (i) a supporting 3D scaffold, (ii) cells (parenchymal and vascular) and (iii) signalling molecules. Specifically, the scaffold, together with integrated signalling molecules, provides structural, biochemical, and biomechanical cues to guide and regulate cell behaviour and tissue development. In the field of liver bioengineering, RM/OBE tries to overcome this limitation by producing bioengineered organs that are capable of supporting hepatic physiological functions, such as drug detoxification, protein synthesis, and the production of bile, which is necessary for digestion. As a corollary, this approach aims to complete the so-called "halfway

technology". Halfway technology has been introduced by Lewis Thomas and refers to a treatment that "represents the kinds of things that must be done after the fact, in efforts to compensate for the lack of understanding of the mechanisms involved in a disease process" [18]. In other words, halfway technology refers to treatments that improve upon symptoms without removing the cause of a specific clinical condition, by managing a disease without proposing a definitive cure able to eradicate the causative agent. In the transplantation jargon, this can be applied to liver transplantation when it was performed in a patient with end-stage liver disease associated with hepatitis C virus (HCV) [19] (before the introduction of Sofosbuvir [20]), or in a patient with colon-rectal metastases [21]. Secondly the life-long needing of immunosuppression therapy may potentially lead to severe acute or chronic toxicity causing additional clinical syndromes [22]. For these reasons the potentially application of RM/OBE as an end-less source of patient-specific organ (and consequently an immunosuppression-free state) could be ground-breaking.

Cell-on-scaffold technology is a cornerstone of RM/OBE obtained by the decellularization technique pioneered by Ott et al. in 2008 [23] who perfused a rat heart with specific chemical detergents (Sodium Dodecyl Sulphate and Triton X-100) obtaining a decellularized "ghost" heart composed just by extra-cellular matrix. This ECM-based scaffold provides not only a structural support with the native anatomy but also important biological molecules that could support cellular proliferation during the recellularization process. These results paved the way for the application of this technology to others organ producing biological, bio-active, three-dimensional organ-specific scaffolds (Fig. 1).
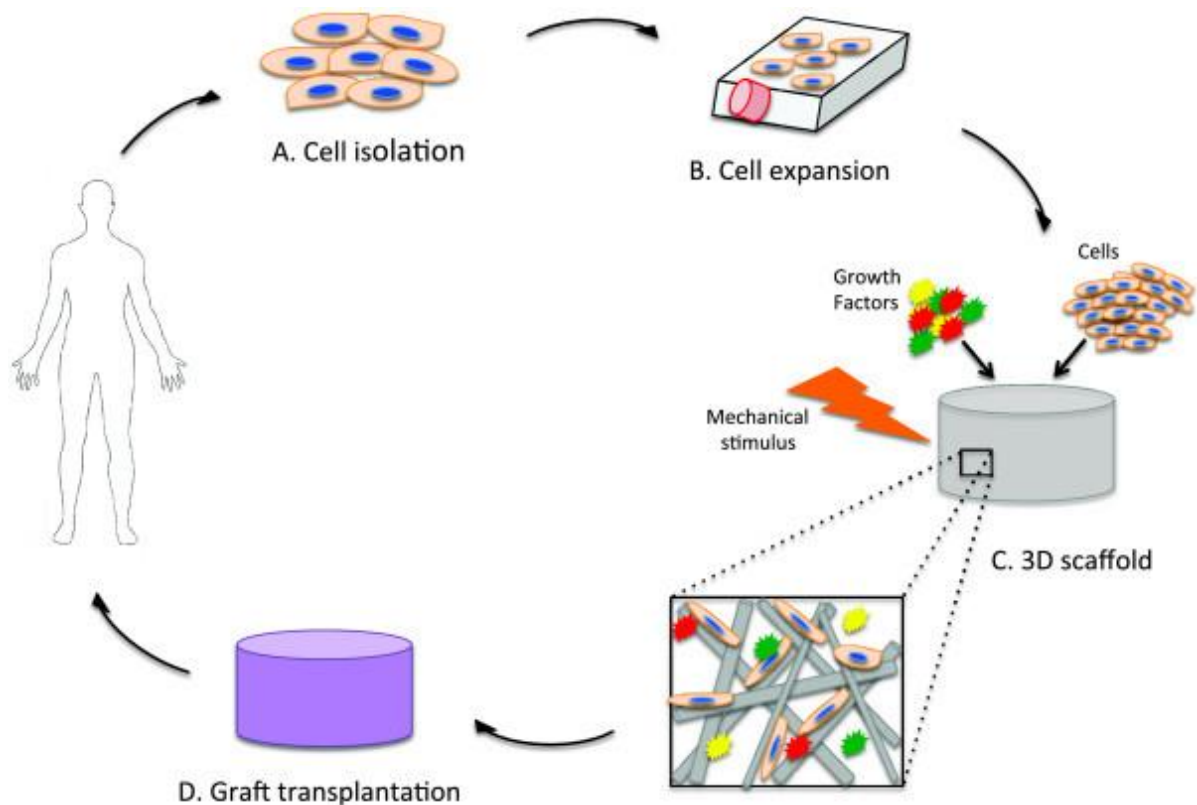
Figure 1 Basic principles of tissue engineering. *A AND B) cells are expanded from an autologous or an allogeneic source. C) A 3D-scaffold is used to support cell growth in the presence of specific growth factors and mechanical stimuli. The combination of scaffold, cells, growth factors, and mechanical stimuli recreates a functional microenvironment that mimics tissue organization. D) The engineered graft is transplanted into a patient.*

[From Serbo J.V., Gerecht S. "Vascular tissue engineering: biodegradable scaffold platforms to promote angiogenesis." Stem Cell Res Ther. 2013]

1.2. The scaffold: The importance of the third dimension for cell growth and proliferation

Even if bi-dimensional (2D) cellular culture has been widely used worldwide for decades, it's considered arguably primitive and does reproducing the real anatomical condition of a tissue. Inserting a third dimension in cell culture is clearly relevant but requires a multidisciplinary approach and multidisciplinary expertise to consider the design of scaffolds for supporting the organisation of cells or the use of bioreactors for controlling nutrient and waste product exchange. The final goal is to create a three-dimensional growth microenvironment mimicking the native tissue as close as possible. At the same

time scaffold should be porous enough to permitting delivering oxygen and nutrients to seeded cells as well as guarantying the physiological outlet of waste cell-derived metabolites [24].

1.2.2. Synthetic scaffold vs biological scaffold

It is well established that cells adapt to their surrounding environment by responding to local signals and cues, via the activation or the suppression of specific pathways, which in turn has consequences for cell proliferation, differentiation and function [25]. In literature, different studies show how a three-dimensional culture condition could enhance the ability of cell growth [26]. As of now, comparison between synthetic or biological scaffold led controversial results with advantages and disadvantages (Table 1) [27]. In recent years, the development of biomaterial production technologies has improved the characteristics of synthetic scaffolds, making them suitable for repopulation process in organ bioengineering. They can be easily sterilized before clinical applications to avoid infections, they are strongly economics and easy of synthesis. In addition, the use of synthetic scaffolds do not require organ donors [28]. A 3D structure can be fabricated starting from diversified biomaterial in order to reproduce physical and chemical proprieties of native extracellular matrix (ECM) that represents the physiologic, native cellular environment. A required characteristic of 3D culture with synthetics biomaterials is to provide an environment that facilitates the nutrient and soluble factor diffusion for a good cell growth since the absence of a dedicated vascular three may bring to the apoptosis of reseeded cells [29]. However, it remains difficult to reproduce the complexity and the dynamicity of the target organs. Biocompatibility is a mandatory requirement for any scaffold. Ideally, a biocompatible scaffold should guarantee cellular adhesion, migration and proliferation with a negligible immune reaction. Limitation of synthetic scaffolds may be overcome by using ECM-derived scaffolds obtained through the organ decellularization. They provide the same environment of native organ, including blood and lymphatic vessel structure [30], active molecules such as peptides and ECM-specific proteins useful for cell growth that are difficult to reproduce artificially [31]. In fact, it has been reported that ECM-bioscaffolds retain specific growth factors,

cytokines and/or chemokines that facilitate cell attachment, tissue integration, remodelling and differentiation.

Table 1: Advantages and disadvantages of synthetic vs biological scaffolds.

	Synthetics scaffolds	**Biological scaffolds**
Advantages	- sterilisable - economical - easy to synthesize - do not require organ donors - no pathogenicity	- sterilisable - native organ structure - active molecules useful for cell growth (peptides and ECM-specific proteins) - not immunogenic
Disadvantages	- cells apoptosis for absence of a vasculature system - difficulty to reproduce the organ complexity - biocompatibility	- organ donors - standardization of optimal decellularization conditions

1.2.3. Synthetic scaffold for liver bioengineering

Synthetic scaffolds play an important role in liver engineering. An ideal synthetic scaffold must be a bioactive substrate capable of reproducing the biophysical and biochemical characteristics of liver ECM. As reported above, synthetics scaffolds should perform a structural support function, promote cell viability and proliferation, and recreate an environment suitable for the diffusion of oxygen, nutrients and cell growth factors [32]. Liver synthetic scaffolds may be manufactured by several types of biomaterials. The material must be biocompatible, biodegradable, non-toxic and it must not generate adverse reactions once implanted in the body. Moreover, using these synthetic sources, no pathogenicity due to animal derived materials would arise. It's also important that the composition, the degradability and the physical properties should be highly reproducible for a large-scale production [33]. Different biomaterials, such as poli-L-lactic acid (PLLA) [34], polyethylene glycol (PEG) [13], polycaprolactone (PCL) [35] and thermoplastic polyurethane (TPU) [36], are considered suitable to create a synthetic scaffold for hepatic bioengineering. Even the technique to produce the scaffold is considered critic. In liver tissue engineering exploiting synthetic scaffolds, the most commonly used are hydrogel-based technology [37], electrospinning [38] nanofibers [11] and 3D-bioprinting [39].

Hydrogels are biocompatible materials that have gained increasing interest, in the last decades, due to their capacity to enhance cell proliferation and biomolecule delivery. Hydrogels are characterized by adjustable chemical and physiological properties. They are categorized by softness and possibility to be conjugated with some proteins, such as collagens and elastin. These properties makes hydrogels more similar to the extra-cellular matrix (ECM) than synthetic biomaterials reported above [29][40]. In a recent study, Ying Luo *et al*. [29] use hydrogel nanofibers to induce spheroid-IPSC to differentiate into hepatocyte-like cells (HLCs). Their results suggest that hydrogel culture system favoured the development of aggregated iPSCs in spheroids. After 11 days of culture, human iPSCs produces spheroids (d = 50-70 μm) with a high vitality of 97.5%. The results showed that hydrogel also promotes the HLCs differentiation of iPSCs with more efficiency respect 2D culture system. In fact, the secretion of albumin, urea production, glycogen synthesis and Cytochrome P450 (CYP450) activity were significantly higher than under 2D condition. Three-dimensional nanofiber scaffolds formed by electrospinning may represent a promising option for tissue engineering liver applications. Nanofibers create an artificial network that mimic ECM. A variety of biodegradable synthetic polymers has been used for scaffold production. For example, PLLA is a biocompatible polymer widely used in tissue reconstruction because of its biodegradability, mechanical proprieties and a non-toxic nature [41].

1.2.4. Extracellular matrix-derived scaffold for liver bioengineering

The use of ECM-based scaffolds is becoming more and more attractive in regenerative medicine and organ engineering strategies, thanks to whole organ decellularization [23][42].
Decellularization consists in the complete removal of cells from tissue or organ [14]. This procedure generates an extracellular matrix-based, acellular, three-dimensional scaffold keeping intact the native organ-specific structure both in terms of hierarchical geometry as well as of bioactive cues. The natural ECM promotes the 3D disposition and orientation of cells and also allows the interaction of cells with the matrix-bound cytokines and growth factors which are preserved after decellularization.

ECM is a very limited compartment within the normal liver. It comprises less than 3% of the relative area on a normal liver section [43]. Nonetheless, ECM is a crucial component. As Mina Bissel states "half of the secret of the cell is outside the cell". ECM is present in portal tracts, sinusoidal walls and central veins making up the three-dimensional structure of the liver.

ECM is the secreted products of each tissue and organ resident cells, representing the ideal scaffold for the repopulation step. Composed by extracellular macromolecules in different concentrations, it provides structural and biochemical support of surrounding cells (Fig. 2). The most abundant ECM protein is collagen. Several isoforms are commonly represented types such as I, III, IV and VI. Each isotype differs in its localization and physical function within the liver. Other major components of the liver ECM are glycoproteins such as elastin, laminin, fibronectin, tenascin, nidogen, and Secreted Protein Acidic and Rich in Cysteine (SPARC). Proteoglycan includes heparan, dermatan, chondroitin sulphate, perlecan, hyaluronic acid, biglycan, and decorin.

The major function of ECM remains the mechanical coherence and resistance of the liver, but liver ECM also has an important role in several biological functions such as cell proliferation, migration, differentiation, and gene expression [44]. In fact, ECM is in a state of dynamic reciprocity with cells, thanks to bioactive molecules that trigger cell–cell communications, cell–matrix adhesion, new ECM formation [45][46] and site-appropriate differentiation of progenitor cells [47]. Biological scaffold provides a unique biochemical profile and set of tissue specific signals that are depend from the native tissue. Consequently ECM-derived scaffold provide cues that influence cell migration, proliferation, and differentiation [14]. This hypothesis has been recently confirmed by a recent study authored by Uygun et al [48], where human liver ECM-scaffolds were shown to retain matrix-bound growth factors such as vascular endothelial growth factor (VEGF), basic fibroblast growth factor (bFGF), hepatocyte growth factor (HGF) and epidermal growth factor (EFG) that play a pivotal role in hepatocyte differentiation and function [49].
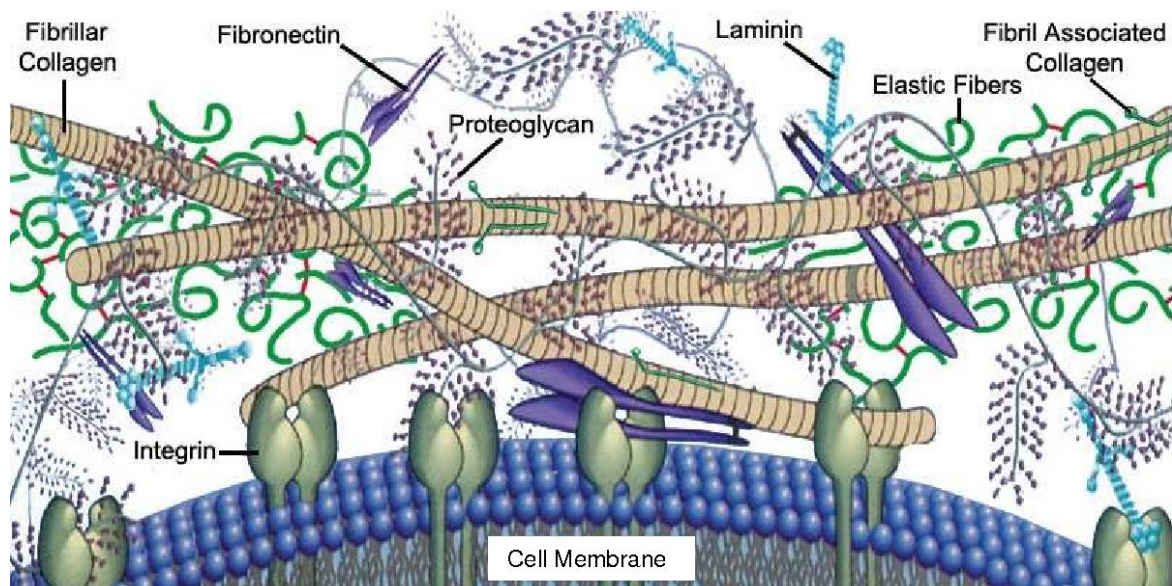
Figure 2: *ECM composition. ECM is composed by several molecules: the most abundant proteins are collagens. The most represented collagen isotypes (I, III, IV and V) varies in its localization and role within the liver. While types I, III, and V, the major constituents of fibrillar collagen, are confined mainly to the portal tract and central vein wall, type IV collagen, in association with laminin and entactin – nidogen, takes part in the formation of a low-density, basement membrane-like material along the sinusoid wall. Other components of the liver ECM are glycoproteins such as laminin, fibronectin, tenascin, nidogen, and SPARC. Proteoglycan includes heparan, dermatan, chondroitin sulphate, perlecan, hyaluronic acid, biglycan, and decorin.*

[*From Joseph M Aamodt, "Extracellular matrix-based biomaterial scaffolds and the host response.", 2016*]

1.3. Decellularization technology

Decellularization could be defined as a process that removes all native cell components to create a three-dimensional extracellular matrix that preserves the native tissue architecture, including the vasculature and ECM molecules. In literature, several protocols based on the different characteristics of tissue and organ, are reported for decellularization. In particular, decellularization can be achieved using physical, chemical or biological agents (Table 2).

Typically, researchers used a mixture of different agents to maximize decellularization effects in order to obtain:

- the lysis of the cell membrane through a physical approach or the use of ionic solutions;

- the separation of cellular components from the extracellular matrix by enzymatic treatments;

- the solubilization of the cytoplasm and nuclear components by chemical detergents.

At least, following decellularization, all chemical residues must be removed to avoid any adverse immune response by the host tissue.

Regardless the decellularization technique a good balance between the cellular removal and the preservation of matrix quality must be pursuit: an excessive decellularization could damage ECM matrix causing biomolecules denaturation and/or the micro-architectural degradation [50]. Therefore, a good combination of cell-detergent contact timing other than detergent concentration should be refined to optimize decellularization and reduce undesirable effects [42].

1.3.1. Physical treatments

Physical decellularization protocols include several procedures that exploit physical strategies in order to remove cell from ECM. Physical treatments destroy the cell membrane allowing the release of cellular content and thus facilitating their removal from the ECM. These methods include freeze/thawing cycle, hydrostatic- based pressure, electroporation, mechanical agitation and perfusion [51].

Freeze/thawing cycles cause cell lysis and membrane rupture in organs and tissues, due to ice crystals formation inside the cells for rapid freezing. Temperature-based decellularization protocols necessitate of multiple freeze-thaw cycles to produce a complete cell removal. Moreover, the resulting membranous and intracellular contents remain if they are not removed by subsequent processing. If, on one hand, this protocol seems to be satisfying for the decellularization, on the other hand, multiple temperature changes could alter the ultrastructure and mechanical properties of ECM [52]. Therefore, this procedure should be used only when such effects are considered "acceptable" in the final ECM product.

The hydrostatic pressure requires a relatively little time, thus being more efficient than detergents or enzymes for cell removal [53]. This method can produce cellular lysis and their removal from the ECM structure, but damage the 3D architecture due to ice crystal formation or to a consequently increase in entropy.

Electroporation involves the application of microseconds electric pulses through the tissue [53]. Thus, the alteration of electrical potential produces the formation of micropores in cellular membrane and therefore cellular apoptosis. However, electroporation method presents some restrictions such as the limiting size of the tissue that can be decellularized and the necessity to be perform in vivo with immune system activation. Nevertheless, if heat generation are controlled, the integrity and morphology of the remaining ECM appears to be retained.

As discussed previously, all physical treatments are not sufficient to obtain a complete decellularization and must therefore be combined with chemical treatments [54]. In particular, mechanical agitation and perfusion were often used in conjunction with chemical treatments to eliminate cellular debris. The achievement of a homogeneous decellularization remains the main issue of physical techniques: in fact, the sample external surface is exposed to a major shacking force and thus, to more detergent compared to the inner portions.

1.3.2. Chemical methods

The effectiveness of chemical agents depends on many factors including cellularity, density, lipid content and tissue thickness. Since all cell removal agents alter the composition of the ECM, one of the goals of decellularization is the minimization of these undesirable effects.

Acids and bases cause the hydrolytic degradation of biomolecules [55]. Several acids are commonly used in decellularization protocols. For examples, Peracetic acid (PAA) acts by removing residual nucleic acids with minimal effect on the ECM composition and structure. Acetic acid (AA) can damages and removes collagens with a corresponding reduction in ECM strength, but it does not affect glycosaminoglycans (GAGs). Sulfuric acid (SA) and ammonium hydroxide (NH_4OH) can destroy cell membranes and intracellular organelles, but at the same time dissociate important molecules such as GAGs from collagen tissues. On the oppose, bases reduce mechanical properties by the cleavage of collagen fibrils and the disruption of their crosslinks. Calcium hydroxide ($Ca(OH)_2$), sodium sulphide (Na_2S), and sodium hydroxide (NaOH) are the most common bases used for decellularization purposes [56]. However, bases can completely eliminate growth factors

from the matrix and decrease of ECM bioactivity. For the above described reasons, acids and bases are not yet commonly used.

Hypertonic solution dissociates DNA from proteins while hypotonic solutions can cause cell lysis by osmotic effects with minimal alterations in ECM molecules and structure. It is common for the tissues to be immersed alternately in several hypertonic/hypotonic solutions cycles in order to obtain a maximum osmotic effect and remove cell residue from within tissue [57].

Non-ionic, ionic and zwitterionic detergents act solubilizing cell membranes and dissociate DNA from proteins [57] [58]. Despite detergents are effective in removing cellular material from tissue, they also cause the disruption and dissociation the ECM ultrastructure. The removal of ECM proteins and DNA by detergents is depending on time, detergent concentration and tissue characteristics. Furthermore, the use of multiple detergents increases ECM protein loss but also allows for more complete detergent removal from ECM after decellularization.

In literature, several detergents are used in decellularization protocols such as Triton X-100 and Sodium dodecyl sulphate (SDS), respectively the most widely used non-ionic and ionic detergent [59]. Triton X-100 is effective in remove cell residues from thicker tissues where enzymatic and osmotic methods are insufficient, with a concomitant loss of ECM proteins and lipidic interaction [60]. On the other hand, SDS more effective for removing cell residues from dense tissue and organs compared to other detergents but is also more aggressive on ECM proteins such as collagen and GAGs.

Zwitterionic detergents present some properties of ionic and other non-ionic detergents, but they have a tendency to denature proteins. 3-[(3-cholamidopropyl) dimethylammonio]-1-propanesulfonate (CHAPS) is a zwitterionic detergent used in decellularization processes due to a good ability to remove cells from thinner tissues, even if it can be ineffective on thicker tissues [61].

When proceeding with chemical methods it is of primary importance to make sure that any chemical residue from the ECM has been removed following the decellularization process. These agents could in fact be toxic to the cells of the host tissue following an in vivo scaffold implant.

1.3.3. Biological agents

Biological agents can be divided into two main categories: enzymatic and non-enzymatic agents.

Decellularization techniques based on enzymatic methods involve the use of enzymes such as proteases and nucleases. Enzymatic agents can interrupt the protein-protein interaction with cellular detachment from ECM basal membrane but also damage the collagen structure of ECM. However, a complete cell removal by enzymatic treatment alone is difficult and enzyme residues may impair recellularization or evoke an adverse immune response [54].

Trypsin is the proteolytic enzyme most used in decellularization protocols. It breaks the peptide bonds at the carboxyl end of the Arg and the Lys. Compared to detergents, it is more disruptive on ECM proteins especially to elastin and collagen, but show a better conservation of GAGs content [62]. Trypsin can be used in order to disrupt tissue ultrastructure and improve penetration of subsequent decellularization agents; in fact, a complete decellularization is difficult to obtain by trypsinization.

Endo/Eso-Nucleases (RNasi and DNasi) cleave the phosphodiester bonds of nucleic acids causing degradation of RNA and DNA [63]. It is necessary to ensure that the enzymatic agents are removed following the decellularization process, as their permanence in the tissue could cause an adverse immune response by the host organism.

Finally, chelating agents, such as ethylenediaminetetraacetic acid (EDTA) and ethylene glycol tetra-acetic acid (EGTA), are non-enzymatic agents used in the detachment of cells from the protein substrate. This happens thanks to their ability to sequestrate metal bivalent cations, such as Calcium (Ca^{2+}) and Magnesium (Mg^{2+}), which are necessary for the cell adhesion bonds to collagen and to fibronectin at RGD receptors. Chelating agents alone are insufficient for superficial cell removal and therefore they are typically used in combination with enzymes such as trypsin or detergents.

It is well known that every decellularization agent and method alter ECM composition and cause some degree of ultrastructure disruption. Minimization of these undesirable effects rather is the objective of decellularization.

Table 2: Commonly used decellularization methods

	Agents	Mechanism of Action	Effect on ECM
Physical treatments	**Freeze/thawing cycles**	Intracellular ice crystals disrupt cell membrane	Disruption or alterations in the ultrastructure of ECM during rapid freezing
	Hydrostatic- based pressure	Burst cells	Can disrupt ECM
	Electroporation	Pulsed electrical fields disrupts cell membrane	Can disrupt ECM
	Mechanical agitation	May rupture cell membranes and but more commonly used to facilitate chemical exposure and cellular material removal.	Can disrupt ECM Ineffective if used alone
	Perfusion	Facilitates chemical exposure and removal of cellular material	Can disrupt ECM
Chemical methods	**Acids** Peracetic acid (PAA) Acetic acid (AA) Sulfuric acid (SA)	Solubilize cytoplasmic components, disrupts nucleic acids and denaturates proteins	Damage collagen, GAGs, growth factors
	Bases Ammonium hydroxide (NH_4OH) Calcium hydroxide ($Ca(OH)_2$), sodium sulphide Na_2S, sodium hydroxide (NaOH)	Solubilize cytoplasmic components, disrupts nucleic acids and denaturates proteins	Damage collagen, GAGs, growth factors
	Non ionic detergents Triton X-100	Disrupts DNA-protein, lipid–lipid and lipid–protein interactions, while is less effective than SDS on protein–protein interactions.	Effective cell removal on thin tissues, Disruption of ultrastructure and removal of GAGs.
	Ionic detergents Sodium Dodecyl Sulphate (SDS) Sodium deoxycholate (SDC) Triton X-200	Solubilize cell and nucleic membrane, dissociate DNA-protein interactions and tends to denaturate proteins	Effectively removes nuclear and cytoplasmic remnants, Disruption of ultrastructure and GAGs
	Zwitterionic detergents CHAPS Sulfobetaine-10	Properties of both non ionic and ionic detergents	Effectively removes cells with mild destruction of ultrastructure in thin tissues
	Hypotonic and hypertonic solutions	Cell lysis by osmotic shock	Not effectively remove the cellular remnants
Biological methods	**Enzymes** Eso/EndoNucleases Protease (Trypsin)	Eso/EndoNucleases catalyze the hydrolysis of terminal/interior bonds of ribonucleotide and deoxyribonucleotide chains, can be useful in the removal of nucleotides after cell lysis in tissues Proteases cleaves peptide bonds on the C-side of Arg and Lys	Prolonged exposure can disrupt ECM structure, removes laminin, fibronectin, elastin, and GAGs Difficult to remove from tissues and can invoke immune response. Incomplete removal of nuclease may also impede recellularization phase. Prolonged exposure of trypsin can damage ultrastructure and distrupt collagens
	Chelant agents	Dissociate cells adhesion to ECM binding bivalent metallic ions	Ineffective when used alone

1.4. Liver whole-organ engineering

To date, perfusion decellularization seems to represent the best option to obtain whole-liver scaffolds. This approach exploits the use of the native vascular tree sensed as the best road to vehicle homogenously the detergent inside the tissue or the organ. Theoretically, this method allows likewise the same contact time between cells and detergent in all the portions of the perfused organ. Perfusion-based decellularization has the big advantage of producing a whole organ scaffold with a size according to the organ source. In lights of this, we are now able to produce small/large animal size liver scaffold [64][65] as well as human whole-hepatic scaffold [66].

The possibility to manipulate a whole-organ liver (or a lobe deriving from it) is essential for transplantation purposes. Several studies indicate that whole-organ decellularization can largely preserve both the native composition and the macroscopic three-dimensional architecture of the liver, ensuring biocompatibility and allowing for extensive recellularization to occur [67]. Preclinical animal models have been established in order to evaluate the efficacy of liver bioengineered starting to small animals models up to human-scale hepatic scaffold (Table 3).

Table 3: Decellularization and recellularization technique in whole-organ engineering

Species	Decellularization technique	Cell source	Recellularization technique	Culture time	Ref
Rat	PV perfusion with SDS	Adult rat hepatocytes	PV infusion in 4 steps	7 days	[48]
Rat	PV perfusion with 1%, 0.5%, 0.25% SDS for 4h each + 1% Triton X-100	Adult rat hepatocytes	PV infusion in 1 step	0.25 days	[68]
Rat	IVC perfusion with 3% Triton X-100/0.5% EGTA	Mouse hepatocytes	Direct parenchyma infusion/continuous PV perfusion/multistep PV perfusion	7 days	[69]
Ferret	PV perfusion with 1% Triton X-100/0.1% NH$_4$OH	Human fetal liver cells + UVECs	PV co-infusion in 16h	7 days	[70]
Rat	PV perfusion with 1% Triton X-100 with 0.05% NaOH vs. 1% SDS	Adult rat hepatocytes	PV infusion in 4 steps	7 days	[71]
Pig	PV perfusion with 0.25% and 0.5% SDS	Human foetal stellate cells + human foetal hepatocytes	PV infusion in 1 step	13 days	[72]

Mouse	PV perfusion with 1% SDS + Triton X-100	Human iPCS	PV infusion	14 days	*[73]*
Pig	PV perfusion with 0.01%, 0.1%, 1% SDS for 24h each + 1% Triton X-100	Porcine hepatocytes	PV infusion in 3 steps	28 days	*[74]*
Rat	SVC perfusion with trypsin, Triton X-100 and EGTA	Rat hepatocytes + rat BM- MSCs	PV co-infusion in 3 steps	6 days	*[75]*
Mouse	1% Triton X-100+0.1% NH$_4$OH	mouse BM-MSCs	PV infusion in 5 steps	28 days	*[76]*
Rat	PV perfusion with Triton X-100 + 0.1% SDS	Human liver stem cells	PV, IVC, SVC and CBD infusion	21 days	*[77]*
Pig	PV perfusion with 1% Triton X-100/0.1% NH$_4$OH	Mouse vascular endothelial cells	PV infusion in 1 step	3 days	*[78]*
Human	IVC perfusion with 3% Triton X-100 + 1% SDS	Human hepatic stellate cells/HepG2/Sk-hep-1	Liver dissected into cubes and injected with cells	21 days	*[66]*
Rat	PV perfusion with 0.01%,0.1%, 0.2% SDS + 0.1% Triton X-100	Adult rat hepatocytes	Direct parenchyma injection in 4 steps	5 days	*[79]*
Rat	PV perfusion with 1% Triton X-100 + 0.1%NH$_4$OH	Human iPSCs hepatocytes	500microm-thick slice of liver scaffold with cell suspension for 20 min	14 days	*[80]*
Rat	PV perfusion with 1% Triton X-100/0.1% NH$_4$OH	Rat liver cell line + human endothelial cell line	PV infusion 1 step + parenchymal injection 10 steps	7 days	*[81]*
Mouse	PV perfusion with 0.1% SDS	Porcine iPSC-heps	PV infusion in 4 steps	5 days	*[82]*
Pig	PV perfusion with 0.1% SDS	HepG2 + human endothelial cell line	PV infusion in 3 steps + 1 step PV and HA	10 days	*[83]*
Rat	PV perfusion with 0.02% trypsin/0.05%EGTA + 1% Triton X-100/0.05% EGTA	Mouse foetal hepatocytes	CBD infusion in 1 step	7 days	*[84]*
Mouse	PV perfusion with 1% SDS + 1% Triton X-100	Mouse hepatocytes	PV infusion in 4 steps	7 days	*[85]*
Mouse	PV perfusion with 4% SDC + 2000 ku DNAse-I	Human ESCS and iPSCs	Liver dissected into lobes and injected directly in 3 points (3x rep.)	13 days	*[86]*
Human	agitation with SDS, Triton X-100, SDC, DNAse	Human hepatic stellate cells/HepG2/ hepatocytes	Seeding/perfusion	14 days	*[87]*
Human	PV and HA perfusion with 4% Triton X-100/1%NH$_4$OH	Human UVECs	Sections seeded in static culture	5 days	*[32]*
Pig	PV perfusion with 1% Triton X-100/0.1% NH$_4$OH	Pig UVECs/ MSCs/ hepatoblasts	PV and HA co-infusion in 2 steps	21 days	*[65]*

Abbreviations: PV, portal vein; SDS, sodium dodecyl sulphate; IVC, inferior vena cava; EGTA, ethylene glycol tetraacetic acid; NH$_4$OH, ammonium hydroxide; NaOH, sodium hydroxide; iHPCs, immortalized mouse fetal hepatic progenitor cells; HA, hepatic artery; SVC, superior vena cava; BM, bone marrow; MSCs, mesenchymal stem cells; CBD, common bile duct; HepG2, liver hepatocellular cells; Sk-Hep-1, human hepatic adenocarcinoma cells, iPSCs, induced pluripotent stem cells; SDC, sodium deoxycholate; ESCs, embryonic stem cells; UVECs, umbelical vein endothelial cells.

1.4.1. Small animal models

Rat liver decellularization has been performed for the first time by the team headed by Uygun BE [48] et al in 2010. The authors, through a single-detergent based, portal vein antegrade perfusion, achieved a whole-liver, acellular, ECM-based scaffold. This technology has been immediately after applied by Shupe et al. [88] with the same results. Uygun et al. perfused the liver with 0.1% SDS alone, whereas Shupe et al. perfused the liver with increasing concentrations of Triton X-100 followed by 0.1% SDS and serum. As with other decellularized whole organs, the liver took on a translucent, white appearance during perfusion in both studies. The investigation by Shupe et al. showed an absence of DNA by hematoxylin and eosin (H&E) and retention of collagen IV and laminin within the ECM. Uygun et al. also showed evidence that DNA was removed and that microvasculature, ECM ultrastructure, and constituents such as collagens I and IV, fibronectin, and laminin were preserved. Hepatocytes were reintroduced into decellularized livers by portal vein perfusion in both studies. Uygun et al. additionally showed preservation or restoration of hepatocyte functions such as synthesis of lactate dehydrogenase and albumin and production of urea persisting up to 8 hours after heterotopic implantation. From this study, some major limitation has been also highlighted such as a perfusion flow-rate too slow to ride the hepatocytes to the inner parts of liver lobes, or the problem of a relative-fast massive intravascular thrombosis leads to the final graft lost. Anyway, from these ground-breaking studies many other applications have been tested both on mice [86][89][73] or rat models [77][80][90].

From the simple concept of decellularization many improvements have been proposed towards a final better decellularization quality seeking for the best balance between a "gentle" decellularization, able to maintain an adequate composition of the micro-environmental condition of the ECM, and an ineffective decellularization leading to cellular and antigenic remnants within the ECM. In 2017 an arterial mono-detergent, arterial liver decellularization has been implement by Struecker B et al. [90] who tested this technology under oscillating pressure conditions. Rat livers were harvested and decellularized in a specific device composed by four chambers connected to each other's and to a pressure distributor, mimicking intra-abdominal conditions during respiration.

Organ were perfused by 1% Triton X-100 (5 ml/minute) detergent via either the portal vein (PV) or the hepatic artery (A) via a 3 hours protocol. Each group was decellularized either with (+P) or without (−P) oscillating pressure conditions, resulting in four experimental groups: (PV − P, PV + P, A − P, A + P; n = 6 for all groups). Arterial liver perfused under oscillating pressure conditions showed a more homogeneous decellularization than livers perfused without oscillating pressure. This result was also associated to a smaller content of remaining DNA per weight with a major content in terms of glycosaminoglycans. Different detergent-based protocols have been also evaluated. In particular, Ren X et al.[91] tested and compared the cellular removal efficacy of two different protocols. Both were based on a portal vein peristaltic perfusion with the inferior vena cava used as fluid outlets, but the first protocol was based on use of 1% SDS whereas the second one exploited a solution of 1% Triton X-100 with 0.05% Sodium Hydroxide. Decellularization conditions were similar with a 37 °C, 2 hours perfusion with a perfusion rate of 5 ml/minute for a total of 600 ml for each sample. Their effects on collagen, elastin, glycosaminoglycans (GAGs), hepatocyte growth factor (HGF) content and influence to the function of hepatocytes cultured in scaffolds were examined and compared. Finally, authors showed that the two decellularization methods successfully removed cells from native liver tissues without any cell nuclei left. At the same time, their effects on the quality of liver ECM were different. Specifically, SDS solution was able to remove most of the collagen whereas around 20% elastin was preserved. GAGs and HGF were largely lost except approximately 10–20% left respectively. In contrast, with Triton X-100-based decellularization, not only most of the collagen, but also 60% elastin, 50% GAGs and 60% HGF were preserved. To test any fallout during the scaffold repopulation authors seeded liver scaffold with a total number of $1.0 - 2.09 \times 10^8$ hepatocytes trough the portal inlet without significant differences in the engraftment efficiency between the SDS (89.7% ± 5.1 %) and Triton X-100 treatment (90.6%±5.7%) (P-value=0.76) detected. In contrast, concerning liver specific functions, including albumin secretion, urea synthesis, ammonia elimination and mRNA expression levels of drug metabolism enzymes Triton X-100 derived scaffolds reseeded with hepatocytes were superior. In conclusion, they concluded that liver ECM scaffolds constructed by perfusion of TritonX-100 could provide a more effective and ideal scaffold for tissue engineering and regenerative medicine approaches.

1.4.2. Large animal models

In this context, towards the clinical translation, one of the most important issue to overcome is to obtain a clinically relevant sized hepatic scaffold to repopulate. As described by Mazza et al. in 2018, the use of large-volume bioengineered tissue or organs drive to different major problems [92]. It requires an appropriate cellular source population and, consequently, a route of administration guarantying the sufficient oxygen and nutrients supply (more complicate to achieve in a higher-volume scaffold). One of the first successful report of porcine decellularized liver scaffold has been proposed in 2013 by Mirmalek-Sani SH et al. [93]. The group adapted a chemical dual-detergent based decellularization, previously used for small-animal model, to decellularize livers from 20-25 kg pigs. Porcine livers were anterograde perfused via the hepatic artery, with chilled PBS, Triton X-100 (3 cycles with increasing concentration: 1%, 2% and 3%) and finally with SDS (0.1%) solutions in saline buffer, with a flow-rate around 50 mL/minute. Histological analysis found the typical loss of cellularity, with a consequent lack of nuclear hematoxylin staining and clearance of cellular cytoplasmic keratins, leaving behind a collagenous-rich, acellular matrix.

Scanning electron microscopy (SEM) confirmed preservation of an intact liver capsule, a porous acellular lattice structure with intact vessels and striated basement membrane. In addition, for cytotoxicity testing, biopsy specimens of decellularized scaffolds were statically seeded with hepatoblastoma (HepG2) cells and cultured for up to 21 days. At different time-points (day 7 and day 21) cells did not exhibit apoptotic markers. Cells were observed attached to the surfaces of matrices, with minimal penetration into the liver matrix scaffold. Additionally, naked hepatic scaffolds were subcutaneously implanted into rodents to investigate scaffold immunogenicity with no noticeable adverse host response surrounding the matrices. This study demonstrated that successful decellularization of the porcine liver could be achieved with protocols developed for rat livers, yielding nonimmunogenic scaffolds for future hepatic bioengineering studies. Continuing in the development of potential clinical applications, Yagi and colleagues [74] confirmed that a dual-detergent protocol (SDS and Triton X-100) can be used to obtain a

porcine liver acellular scaffold preserving the ultrastructural extracellular matrix components, the functional characteristics of the native microvascular and the bile drainage network of the liver, as well as important growth factors necessary for angiogenesis and liver regeneration (HGF, bFGF, VEGF, IGF-1). Interestingly, the group repopulate the scaffold with 1×10^9 hepatocytes by an intra-portal multistep infusions. Prior to the perfusion culture experiments, the liver scaffold was decontaminated by ultraviolet irradiation and finally transferred to a customized organ culture chamber basically consisting in a peristaltic pump, a bubble trap, and an oxygenator. The system was placed in an incubator for temperature control at 37 °C, and the oxygenator was connected to atmospheric gas mixture. After cellular infusion the graft was continuously perfused through the portal vein at 4 ml/minute with continuous oxygenation that delivered an inflow partial oxygen tension of around 300 mmHg. The medium was changed daily. Twenty hours after the infusion, more than half of the attached cells in the decellularized liver scaffold (attached cells: 74% ± 13% of infused cells) were found in the portal vein but they had moved into the parenchymal space at day 4. Albumin staining after 4 and 7 days of culture-perfusion showed that hepatocytes engrafted around the larger vessels, repopulating the surrounding parenchymal area. The amount of immunostaining albumin of engrafted hepatocytes after 4 days of the perfusion culture was similar to that in normal livers; however, the expression decreased considerably after 7 days in the perfusion culture. These results determined how porcine primary hepatocytes could efficiently be delivered in a large-scale liver bioscaffold, providing important insights towards the creation of a human-sized bio-engineered liver. More recently, in 2015, Struecker et al. presented a decellularization technology based on a pressure control protocol [94]. The group proposed an accelerated (7 hours overall perfusion time) and effective protocol for human-scale liver decellularization by pressure-controlled perfusion with 1% Triton X-100 and 1% sodium dodecyl sulphate via the hepatic artery (120 mmHg) and portal vein (60 mmHg). The proprietary perfusion device allowed generating specific pressure conditions mimicking the intra-abdominal conditions during respiration, optimizing, in this way, the micro-perfusion within the liver and, so on, the homogeneity of the whole decellularization process. Uncommonly, the same group will presented a version designed to a small animal model only two years later [90]. The increasing interest for the organ bioengineering required preclinical research in large

models to demonstrate the feasibility also concerning the implantation of decellularized/recellularized liver scaffolds. In their article, Ko et al. [78] focused on the process of reendothelializing livers following whole organ perfusion decellularization using Triton X-100 and ammonium hydroxide. Rather than relying on endothelial cells to passively attach to native matrix, the investigators actively facilitated their attachment by treating the scaffolds with 1-ethyl-3-(3-dimethylaminopropyl)-carbodiimide/N-hydroxysuccinimide (EDC/NHS), and by perfusing anti-CD31 antibodies through the vasculature. With these antibodies in place, endothelial cells were infused using both static and perfusion culture methods. Not surprisingly, scaffolds that had been reendothelialized using this method showed improved patency and resistance to platelet adhesion compared to acellular scaffolds. As a result, reendothelialized livers implanted into a heterotopic porcine model were able to withstand physiological flow for 24 hours. Moreover, this study demonstrated for the first time, the feasibility of the implantation of a large-scale decellularized/reendothelialized scaffold in a large animal recipient. While a much longer time span will be necessary for therapeutic purposes, this article demonstrates how engineering strategies can be used to deliver new cells to specific regions within decellularized organs.

The extensive exploitation of pig livers is related to both their wide availability and dimensions in a range compatible with the size of human liver and, for this reason, several research groups have investigated their application for liver bio-engineering [72][96][97] [98].

1.4.3. Human tissues

Even if the use of xenogeneic livers, derived from different species, is largely proposed and deeply discussed as template for clinical application, major concerns have been raised in particular based on three-dimensional architectural differences, on biocompatibility and on immunogenicity. Above all, the difference in vascular structure between human liver and liver collecting from animal species could lead to hemodynamic consequences incompatible with the preservation of the transplanted engineered liver tissue. Indeed, the ideal biomaterial should be derived from human liver. Following this

concept, in 2015 Mazza et al. [66] applied for the first time, the decellularization to a whole human liver successfully obtaining a human whole-liver acellular ECM-based scaffold. The decellularization protocol consisted in a perfusion regime based on perfusion repeated cycles of distilled water (dH_2O), para acetic acid (PAA) and ethanol hydroxide (EtOH), preceded by a single cycle of freezing/thawing. Histological stainings (H&E, Sirious Red and Elastin Von Gieson) demonstrated, in the decellularized samples, the complete cellular removal with the preservation of collagens (type I, III, IV), fibronectin and elastin. Ultrastructural characterization by SEM confirmed also the preservation of the three-dimensional micro-anatomy of the portal tract with a surrounding honeycomb-like pattern. The group faced the interspecies biocompatibility of the scaffold through the subcutaneous implantation of $125mm^3$ cubic ECM scaffold fragments in immunocompetent C57BL/6J mice and finally evaluated at 7 and 21 days post-implantation. Polymorphonuclear cells and lymphocytes were observed at 7 days post-implantation, indicating a mild inflammatory response. Inflammatory cells were mostly seen in the tissue around the implants. By contrast, at 21 days post-implantation, little or no inflammatory infiltrate was observed around the implants. These same results were confirmed also by the omental implantation of the scaffold fragments, indicating a progressive host cell infiltration and arteriolar neovascularization. Although further studies are needed it must be stress out how biocompatibility rests a crucial issue to be clarified when proposing bio-technologies potentially leading to Advanced Therapy Medicinal Products (ATMP) [99]. Human-liver cubic scaffold have been also statically seeded by LX2, HepG2 and SK-Hep1 cells (for a total amount of 2×10^6 cells). Seeded scaffolds were kept for 2h in a humidified environment at 37 °C with 5% CO_2 allowing cell attachment followed by addition of complete culture medium up to 21 days post-seeding. H&E and Ki67 stainings showed that all cell types were able to repopulate liver scaffolds while still proliferating at 21 days. Cellular well-being was also confirmed by the total cell count in human liver scaffolds repopulated with LX2, HepG2 and Sk-Hep-1, that increased significantly between 7 and 14–21 days.

Again, the same group, proposed a new decellularization protocol based on the application of high shear stress determining an acceleration of cellular removal from human livers [87]. In this case the decellularization has been focused on liver cubes

samples. After a first perfusion with 1% PBS in order to eliminate blood livers were frozen at −80 °C for a minimum of 24 hours to assist with the destruction of the cellular membrane. Afterwards, human livers were thawed at 4 °C overnight, cut into 125 mm^3 cubes and undergone a cycle of freezing/thawing. Once thawed the cubes were transferred into 2 ml safe-lock tubes and an increasing g-force intensity (45g) has applied with an orbital shaker. With this setup, 3 hours of shaking have been enough to obtain acellular liver scaffold cubes (against to 36 hours of the previous perfusion protocol). After decellularization, histological analyses assessed the elimination of nuclear as well as cellular material with simultaneous of collagen and elastin. Micro-anatomy, biochemical and biomechanical properties have been evaluated and certified. At SEM decellularized liver cubes showed the preservation of a portal tract, collagen fibrils and hepatocyte pockets. The ability of ECM scaffolds to attract blood vessels and to promote neo-angiogenesis has been demonstrated by employing the chicken chorioallantoic membrane (CAM) assay in several studies with the formation of newly blood vessels in a spoked-wheel patterns close to the scaffold.

Latterly, Verstegen et al. [32] continued exploiting the use of human livers that are deemed medically unsuitable for transplantation due to poor condition, as a potential source for the generation of bio-engineered hepatic scaffolds. Aiming to perform whole liver decellularization in a clinical series, they proposed the use of a dual perfusion through the portal vein and hepatic artery by a custom-made controlled machine, able to produce a mild non-destructive decellularization protocol. This protocol has been demonstrated effective in 11 discarded human whole liver grafts to generate constructs that reliably maintain hepatic architecture and ECM components using machine perfusion, while completely removing cellular DNA and RNA.

Although excellent results have been reported in literature concerning the use of human liver as base for hepatic bioengineering, a lot of work is still to be made and future developments for in-vitro recellularization may be achieved by the use of innovative and dedicated bioreactors to better recreate the hepatic physiological microenvironment.

1.5. Recellularization technology

To create an organ suitable for transplantation, the decellularized scaffolds should be repopulated with suitable functional cells able to perform all the organ-specific task. Specifically, this seems to be for liver due to the multitude of different rules that it's realises, including above all, metabolic processes and albumin and cholesterol production.

Scaffold recellularization is a crucial step in organ bioengineering where cell type, sources, number and seeding methods need to be well evaluated [100]. Recellularization of whole liver is progressing. Although recapitulation of sinusoids is underway with hepatocytes, which account for about two third of the whole liver volume [101], regeneration of the biliary tree on liver ECM has proved to be more difficult.

It is reported that hepatocytes are physiologically able to reconstitute liver structures and organ functionality after damage [102]. For these reasons, primary hepatocytes could represent the first-line choice for recellularization of liver ECM scaffold. Nevertheless, due to their limited proliferative ability, hepatocytes *in-vitro* maintaining and expanding seems to be difficult, being possible only for a few weeks [103]. Moreover, once plated, these cells gradually lose the typical morphology as well as the liver specific functions such as protein synthesis, carbohydrate metabolism and cytochrome P450 activity in a process called dedifferentiation. Finally, if the goal is to create a totally immunological human compatible organ to avoid rejections, hepatocytes need to be freshly isolated from the recipient patient. In fact, it has been described that after hepatocyte transplantation, recipient may undergo inflammatory reaction and immune rejection in the first 24 hours [104].

In the last years, several efforts were made to find another source of cells for scaffold repopulation. Stem cells are encouraging substitutes for primary hepatocyte because of their self-renewal capacity and their ability to give rise to different type of cells [105]. In literature, several protocols using stem cells are described to reproduce functional hepatocytes. These methods are based on addition in culture medium of specific soluble factors such as growth factors, transcriptional factors and cytokines [106]. Moreover,

evidences displayed that the differentiation of stem cells into mature hepatocyte is more efficient on 3D scaffold compare with 2D condition [107][108][109]. Despite the several efforts, the different stem cells used for recellularization, can give unlimited number of hepatocyte-like cells (HLCs), but with incomplete functions [110].

1.5.1. Cell sources

HLCs used in liver bioengineering can be generated from:

- Embryonic stem cells (ESCs)

- Hepatic progenitor cells (HPCs)

- Foetal stem cells

- mesenchymal stromal cells (MSCs)

- induced pluripotent stem cells (iPSCs).

1.5.1.1. Embryonic stem cells (ESCs)

ESCs are pluripotent stem cell derived from inner cell mass of blastocysts [111]. The differentiation in specific cell types starts from the formation of three germ layers: endoderm, mesoderm, and ectoderm. ESCs could be cultured indefinitely in undifferentiated state. ESCs can differentiate *in vitro* into hepatoblasts in presence of specific stimuli and gain expression of characteristic liver cellular markers [112][113][114]. However, there are ethical limitations for their use, and they are characterized by the loss of epigenetic modifications, which could develop in teratomas [115].

1.5.1.2. Hepatic progenitor cells (HPCs)

HPCs are classified as adult stem cells, partially hepatic committed. HPCs present a greater regenerative capacity than adult hepatocyte and have a physiological rule in liver tissue repair after damage. They naturally show bipotential differentiation ability in both hepatocyte and cholangiocytes, two main epithelial liver cell types [116]. HPCs can be isolated and expanded from discarded livers. They are difficult to isolate due to the

absence of specific markers. Khuu et al [117] described that after *in vitro* differentiation, HPCs express albumin (ALB), alpha fetoprotein (AFP) and cytokeratin 18 (CK18) supporting their hepatic commitment. Wang et al. [67] demonstrated that human hepatic stem cells seeded onto liver specific biomatrix scaffold in presence of specific stimuli, lost stem cell markers and differentiated into mature liver parenchymal cells.

1.5.1.3. Foetal stem cells

Foetal stem cells are multipotent cells that under specific stimuli are able to differentiate in hepatocytes and cholangiocytes [118]. They can be isolated from foetal tissues as well as from foetal blood and BM. They show higher clonogenic and lower immunogenic potential *in vitro* than adult stem cells [119]. Moreover, the differentiation potential seems to be greater than adult counterpart. Several studies show the ability of foetal stem cells to give rise to HLCs. Baptista et al [70] reported that hepatoblasts seeded onto bioscaffolds differentiated into the biliary and hepatogenic lineage. Zhang et al [120] obtained HLCs from human foetal stem cells, that gained *in vitro* functional activity such as albumin production, glycogen storage and CYP450 activity. However, the limited cell number that could be obtained and the ethical issues that arose from the use of foetal stem cells represent great limits for their applications [119].

1.5.1.4. Mesenchymal stromal cells (MSCs)

Recently, MSCs have been reported as an appropriate cell source for liver bioengineering. MSC are multipotent stem cells that give rise to many mesodermal cells (Fig. 3). They can be isolated from different sources such as bone marrow, umbilical cord blood, adipose tissue, liver, spleen, trabecular bone, pericytes and articular cartilage [121]. Advantages of using MSC in tissue regenerative medicine include an easy isolation, a high proliferative capacity and finally the potential use of autologous cells. Human MSCs have been reported to be able to differentiate in HLCs after appropriate stimuli addition in culture medium [122][123]. Moreover, MSCs can stimulate the regeneration of endogenous parenchymal cells and enhance fibrous matrix degradation [124]. In addition, there are no

ethical or tumorigenic issues. Recently, Li et al [125] explored the effect of hepatic differentiation of human derived umbilical cord blood MSC seeded on decellularized liver scaffold. The expression of hepatic gene markers such as albumin, CK-18, Hepatocyte Nuclear Factor 4 (HNF4) and CYP1a2 and CYP3a4 were upregulated after 25 days of induction protocol, while stem cells specific genes such as Oct-4 and Sox2 were downregulated. Moreover, MSC derived HLCs gained liver-specific functions such as albumin secretion, glycogen storage and ammonia conversion to urea.

### 1.5.1.5.   induced pluripotent stem cells (iPSCs).

iPSCs derived from somatic cells reprogrammed to pluripotent state are being widely explored as an alternative to primary human hepatocytes for their capacity to differentiate *in vitro* into HLCs in presence of specific stimuli [126]. iPSCs present the same level of pluripotency as ESCs and constitute an unlimited cell source that give rise to both parenchymal and supportive cells [127]. Furthermore, iPSC technology in organ bioengineering has the advantage to create a patient-specific cell-therapy [128]. The use of iPSCs, have no ethical problems and do not induce host immune rejection [129].

At first, Yamanaka et al [130] demonstrated that both mouse embryonic and adult fibroblasts could be genetically reprogrammed to create iPSC by the retroviral transduction of four reprogramming factors (Oct4, Sox2, Klf4, and c-Myc genes). Currently, there are different protocols to create iPSCs based on non-integrating genomic modifications, protein introductions, and use of chemical agents [131][132]. Recently, Jaramillo et al [49] evaluated the effect of decellularized human liver matrix (hDLM) to increase the efficacy of a differentiation protocol towards HLCs. In this culture condition, functional hepatic markers were upregulated and hepatic transcription and nuclear factor expression was similar to those of primary human adult hepatocytes. However, despite these cells may represent an ideal source for repopulation, the HLCs derived from iPSCs are still not functional equivalent to primary hepatocytes. In addition, the tumorigenic potential of iPSCs must be evaluated.

In 2019, Kehtari et al [133], used as an alternative scaffold to circumvent the donor shortage, a differentiation protocol to obtain hepatic differentiation of hiPSCs seeded on

decellularized Wharton's jelly scaffolds (DWJS). After differentiation, the cell size increased slightly and showed the typical morphological feature of hepatocytes. Moreover, the expression of human liver specific genes, such as albumin, CK-19, TAT, and Cyp7A1 were significantly increased in cells cultured on DWJS compared with 2D controls. Furthermore, albumin secretion and urea synthesis were assessed to test the functional and metabolic activity of hiPSCs derived hepatocyte. Despite hepatocyte-like cells in DWJS exhibited more abundant and stable metabolic activities than those cultured in culture plates, also in this case iPSCs presented lower functional abilities compared with primary hepatocyte.
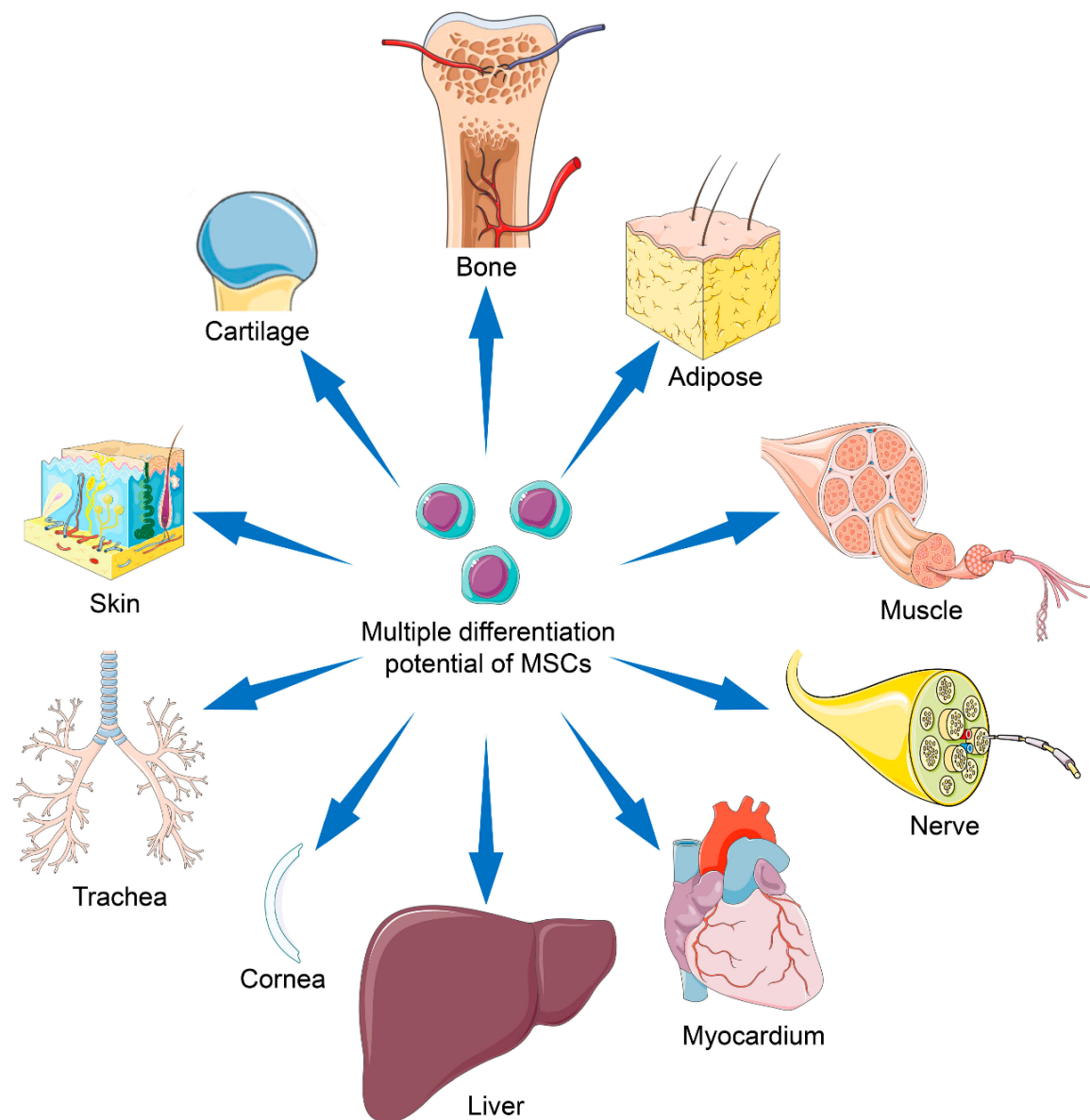
Figure 3: Applications of mesenchymal stem cells with multiple differentiation potential for repair of various tissues. The MSCs can be easily extracted from varies tissues, and the multilineage differentiation and immunoregulatory properties of MSCs make them an ideal cell therapeutic candidate in regenerative medicine.

[From: Yu Han et al, "Mesenchymal Stem Cells for Regenerative Medicine.", Cells 2019]

1.5.2. Cell seeding strategy

Recellularization efficiency is also influenced by seeding methods and cells number. Since hepatocytes are able to regenerate, a number of cells between 1 and 10% of native liver mass are enough for organ reconstitution [134]. In addition, the need arises to maintain the different cell type proportions to guarantee a physiologically functional organ.

Scaffold may be repopulated by different cell type following different seeding methods. The commonly methods use for recellularization includes direct parenchymal injection, multistep infusion and continuous perfusion. Soto-Gutierrez et al [69] tested these methods and determined that the efficiency with multistep infusions was higher than with direct parenchymal injection or continuous perfusion. In another study, Uygun et al. [48] evaluated the efficiency of mouse hepatocyte reseeding into decellularized rat livers, using direct parenchymal injection, continuous perfusion or multistep infusions. After extensive evaluation of the integrity, attachment, function, and distribution of engrafted cells, it was found that the multistep infusions technique presented the most suitable results.

Recently, bioreactors are receiving growing interest as a strategical tool to preserve recellularized whole-liver scaffolds [135]. Bioreactor is a type of organ-perfusion system that provide a continuous supply of nutrients and oxygen while simultaneous removing metabolic wastes. Ideally, bioreactor system should be capable to maintaining a fully recellularization in a whole-organ scaffold in term of temperature, perfusate, chemical factors and mechanical environment. Several factors such as flow rate and perfusion should be well defined as they have a major impact on tissue growth.

A critical aspect of the recellularization, is determined by the loss of organ endothelial layer due to the decellularization process. In absence of such cells, coagulation can initiate when blood is exposed to matrix proteins. For this reason, it is essential to develop strategies that improve the hemocompatibility of the scaffolds and avoid blood clotting in vascular system of transplanted animal model. Based on these observations it has been described a co-culture system of vascular cell type with MSC in order to obtain a vascularized tissue construct [136]. Hussein et al. [83] developed a heparin-gelatine mixture to cover vascular surfaces in decellularized porcine livers. After coating of blood vessel, scaffolds were reseeded with endothelial cells (EA.hy926) and subsequently with epithelial cell derived from hepatocellular carcinoma (HepG2). Their results demonstrate that heparin-gelatine gel supports the attachment and migration of endothelial cells.

1.6. Future applications

1.6.1. 3D bio-printing of human hepatic tissue using liver extracellular matrix as bio-ink

Three-dimensional bio-printing is the combination of 3D printing and tissue engineering through the use of bio-materials, bio chemicals and living cells as "ink". The goal of this growing field of research is the reproduction of tissues or whole organs for drug development and testing, diseases modelling and, most of all, regenerative medicine. So far, 3D bio-printing technology has been exploited for the development of many in vitro tissues, including skin [137][138], nerve grafts [139] cardiac tissue [140], vascular tissue [141], bone tissue [142].

The currently in-use bio-ink is a hydrogel solution with cells suspended in it: the challenge is the development of a hydrogel with characteristics as similar as possible to the natural ECM, which varies from tissue to tissue.

Despite the different preparations tested up to now, a perfect combination hasn't been found. Naturally derived bio-inks (like agar, agarose, collagen, gelatine, alginate, chitosan, hyaluronic acid, fibrin/fibrinogen) have a low viscosity which make them not suitable for bioprinting. Synthetic materials (like polyurethane, polyethylene glycol, and polylactic acid) on the other hand, have tunable mechanical properties and cross-linking capacity but they are not adequate for cells adhesion, growth, differentiation, survival and function. Therefore, the decellularized ECM has been introduced as an alternative bio-ink source.

The advantages of using animal or human ECM is the maintenance of tissue microenvironment with retained growth factors and cytokines which act as biological cues for cellular activities. Furthermore, the native ECM is capable to induce tissue repair and avoid antigenicity reactions of the host tissue against the graft [92][143]. Bio-printed tissue with dECM has also been shown to have a biodegradation rate equivalent to that of the same in-vivo tissue, balanced with the cells capability to secrete new ECM. The main problems with decellularized ECM are the rheological properties, which are important for cell survival during the extrusion phase and for the preservation of the shape of the printed module. dECM is soft and with poor mechanical properties. However, it has been

demonstrated that vitamin B2 addiction or UVA radiation can induce covalent cross-linking allowing for tuning of the mechanical behaviour [144]. For what concerns liver, Lee et al. [145] developed in 2017 a liver decellularized ECM for 3D bio-printing. In this study, a porcine liver was decellularized, lyophilized and ground into powder. The powder so obtained was then solubilized by pepsin digestion with 0.5 M acetic acid and centrifuged to remove undissolved particles, which would have eventually blocked the nozzle of the 3D printer. Lastly, liver dEMC solution was neutralized to obtain a pH favourable for cells encapsulation; human bone marrow-derived stem cells were used. The dECM showed excellent print ability without significant cell death during the printing phase. Four liver specific transcription factors (HNF1A, HNF3B, HNF4A and HNF6) were analysed and compared to those expressed by the same stem cells encapsulated in a collagen bio-in showing an enhanced stem cell differentiation in the dECM [146].

1.6.2. Three-dimensional organoid

1.6.2.1. The organoid culture environment: the concept of stem cell-driven tissue engineering

A new strategy for regenerate functional and transplantable liver graft is based on liver organoids. Organoids are defined as an organized three-dimensional structure derived from different stem cell in which cells spontaneously self-organize into multiple functional cell types or progenitors, acquiring some characteristic functions of native tissue [147][148][149][70]. In this way, organoids mimic in vivo structure and complexity of an organ.

Organoids could be obtained from fresh or frozen patient biopsies, with low-invasive techniques [150]. Several characteristics make adult human liver organoids suitable for cell therapy approaches. In particular, i) they have an extensive degree of clonogenic potential, ii) cells maintain the ability to differentiate into hepatocytes or cholangiocytes in organoid culture condition, iii) proliferating cells could be maintained for months without genetic transformation (genetic stability) iv) a significant number of cells can be obtained from a small number of starting cells like in specimen of liver biopsies.

However, there are disadvantages such as the difficulties in cells standardizing culture and ethical issue for ESCs derived organoids. Moreover, the lack of vasculature system, stromal cells and immature cells.

Organoids can be produced by different strategies [150]:

1.   differentiating cells on-bed of feeder cells or an ECM-coated surface,

2.   using of mechanically assisted culture for primer tissue differentiation,

3.   forming embryoid bodies on low adhesion plates or over hanging drop culture system,

4.   using floating culture of embryoid body-like aggregates on the low adhesion plates in serum free-condition.

Recently, Huch et al. [149] reported that in specific organoids culture condition, p-Leucine-rich repeat-containing G protein coupled receptor 5 (Lgr5) positive cells under the influence of Wnt signalling, spontaneously self-organize into specific structure called cyst-like organoids. These structures mimic the functionality and the cellular composition of liver tissue and can be maintained in vitro for several month to few years. Cells in the 3D liver organoid in a specific medium could differentiate into hepatocytes or cholangiocytes. Upon hepatocyte differentiation in organoids, cells gain hepatic morphology and present an upregulation of typical hepatocyte and ductal marker. Moreover, organoids show some hepatic function like glycogen storage, albumin production and LDL uptake, although to a smaller degree than mature hepatocyte.

1.6.2.2.   Patient-derived organoids for personalized applications

Organoid technique might be useful in different clinical applications such as disease modelling, drug screening and in clinical implantations.

To date, several studies such as drug efficacy and safety are performed on animal disease models. Recently, the develop of 3D-liver stem cell cultures organized in organoids opened new options in this field [151], allowing to evaluate some pathological aspect without the use of more expensive and time-consuming animal models. In fact, cells

expanded from patients with genetic liver disease maintained also the disease phenotype in culture.

Autologous transplantation of genetically corrected organoids from patients with metabolic disease could be another therapeutic application of liver organoids. To this regard, Huch et al. [148] demonstrate that organoid derived from patients with alpha1 antitrypsin deficiency (AA1T-D) reproduce in their structure the same misfolding and aggregation of AA1T protein of hepatocytes.

Moreover, Nantasanti et al. [152] obtained gene correction by transferring the functional copper metabolism domain containing 1 (COMMD1) gene to COMMD1 deficient organoids obtained from dogs with autosomal recessive COMMD1 deficiency, as Wilson's disease model.

In particular, liver organoids have been used to study monogenic disease of epithelial compartment [153]. However, in clinical applications, genetically corrected organisms might cause graft rejection and for this reason, a short-term immunosuppressive therapy are recommended despite autologous transplantation, to avoid immune reaction to non-self-proteins in transduced organisms. Moreover, the genetic instability might increase the risk of tumor formation following transplantation [148].

Organoids provide an alternative method to study liver disease, suitable for personalized medicine. Currently, the possibility of using hepatic organoids in cell therapy is encouraging but requires further verifications before being able to use it in clinical setting.

1.6.3. Bioengineered ECM-derived livers as a new tool for drug testing

An ideal model for pharmacological testing should have two characteristics: it must resemble as close as possible a human being and at the same time it must preserve the integrity of the tested subject. Animal models have been consistently used but, due to the considerable inter species variability, together with the ethical and financial issues, they were not found to be ideal for toxicological and pharmacological drug testing. At present time, the recognized gold standard for in vitro testing of drugs is primary culture of human hepatocytes.

To allow for an optimal phenotypic gene expression and response to drugs, histological and physiological hepatocyte conditions, as well as their interaction with one another, should be maintained in in-vitro studies. To recreate these conditions different configurations of extracellular matrix and medium have been tested. However, the reproduction of a natural-like ECM is a challenge due to the large variety of constituents produced by the different cell types of the liver. In such cultures, cells tend to lose their morphology and integrity with time: after approximately two weeks hepatocytes deteriorate due to cytoskeleton alterations which subsequently cause changes in the signalling pathway and, eventually, in the phenotypic gene expression [154]. The result is a down regulation of drug-metabolizing enzymes, reducing the relevance of the testing. To overcome these limitations bio-engineered livers could be used in the nearer future for research purposes [67][155][156]. Liver bio-scaffolds have been seeded with both mature hepatocytes and stem cells. Hepatocytes plated on decellularized liver scaffolds have significant advantage compared to primary culture of hepatocytes. The natural ECM not only promotes the 3D disposition and orientation of cells but also allows the interaction of cells with the matrix-bound cytokines and growth factors which are preserved after decellularization. In these conditions, hepatocytes have been found to attach faster to the bio-matrix (few minutes versus hours in type I collagen) and remain fully functional and morphologically stable longer (8 weeks versus 2 weeks on collagen type I) [67].

The preserved 3D architecture and native composition of the decellularized liver scaffold are able to drive differentiation of seeded stem cells toward adult liver fates. Stem cells have self-renewable ability, high proliferative potential and the possibility to differentiate in multiple cell lineages: these features give this *in vitro* liver model a constant availability of cells allowing longevity of the culture and presence of hepatocytes together with biliary epithelial cells [157]. A study investigated the so-generated liver by exposing it to six drugs, well-known for targeting specific CYP enzymes, and found that it provided enhanced activities of metabolic enzymes compared to the 2D-culture condition [158]. In summary, it was concluded that liver scaffolds 'better represent the natural in-vivo environment in an *ex vivo* system' [71] offering tremendous opportunities for drug development and testing. Furthermore, the use of patient-derived stem cells allows the possibility to test patient-specific response to drugs.

1.7. Future perspectives

The main goal of liver bioengineering remains to provide new functional organs for clinical translation in order to overcome the shortage of organ donors. Currently, to achieve this purpose several challenges need to be met. Within this journey towards bioengineered organs, there are three fronts in the preclinical setting on which to work: (1) scaffolding; (2) recellularization; and (3) cell signaling. The investigations concerning the ECM reveal that a state of dynamic reciprocity between cells and ECM exists. It will therefore be necessary to discover the complex and delicate dynamic equilibrium between the cells and ECM, allowing the generation of new organs. In particular, a more detailed decellularization process, an optimization of organ-specific recellularization techniques, a better cell differentiation capacity, and a more exhaustive understanding of the interaction between cells and ECM will play an essential role in the progression of this research field. Moreover, scaffold-based organs and 3D printed organoids provide an alternative method for studying liver disease and are suitable for personalized medicine. Currently, the possibility of using hepatic organoids in cell therapy is encouraging but requires further verification in clinical settings.

Therefore, the great challenge for the next years will be the translation to the clinical setting that will hinges on how effective we will be in understanding "the bench phase".

2. AIM

Allogeneic liver transplantation is still considered the gold standard solution for end-stage organ failure; however, shortage of donor organs has resulted in extending transplantation waiting lists. To overcome the lack of donors it is mandatory to develop new therapeutic options.

In the last years, organ bioengineering has been extensively explored to provide transplantable tissues or whole organs with the final goal to create a three-dimensional growth microenvironment mimicking their native structure. In literature, it is well reported that Extracellular matrix (ECM) based scaffold provides structural support and important biological molecules that could help cellular proliferation during the recellularization process.

In the present study, we decellularized pig livers and then repopulated them with allogeneic porcine mesenchymal stromal cells (pMSCs) to study the interaction between pMSCs and liver specific ECM. The final aim was to understand if ECM can influence and/or promote pMSCs toward differentiation into hepatocytes or hepatocyte-like cells without specific growth factor in culture medium. Our experimental design was divided into different steps in order to define:

•   the optimal liver decellularization strategy;

•   the isolation, expansion and characterization of pMSCs;

•   the recellularization strategy of ECM;

•   the liver specific functions in pMSCs cultured on native ECM.

3. MATERIALS AND METHODS

3.1. Animals.

Female Large White 6 months old piglets (mean weigh 30 ± 5 kg) were used for both liver harvesting and bone marrow (BM) collection. Animals were pre-medicated with intramuscular injection of tiletamine hydrochloride-zolazepam hydrochloride (10mg/kg), subsequently their marginal vein of the ear was cannulated and the anesthesia induction was performed with propofol (0,2 mg/kg EV). Anesthesia was maintained during surgery with a continuous infusion of propofol (10 mg/kg/h EV).

The surgical procedures were performed in the fully equipped animal research laboratory of Experimental Surgery, University of Pavia (Fig. 4).

Figure 4: Photograph of the operating room of the Experimental surgery laboratory, University of Pavia. The surgical procedure has been carried out in fully sterile conditions. Porcine livers were obtained using a surgical technique similar to the one used for multi-organ explant in a human cadaveric donor.

3.2. Liver retrieval procedure.

The surgical procedure has been carried out in fully sterile conditions. A vertical midline laparotomy was used to get access to the abdominal cavity. The liver was retracted ventrally and superiorly, and the posterior diaphragmatic attachments of the liver were divided to gain complete mobilization of the organ. The hepatic hilum was isolated, its elements identified, and a band left in place as landmark. The IVC and the aorta were isolated. The aorta was ligated just above the iliac bifurcation and cannulated. After an intravenous injection of heparin (100 U/kg), heparinized Sodium chloride solution (0.9% NaCl, Baxter) was infused in the aortic cannula while the IVC was transected and the aorta was clamped just under the diaphragm. During perfusion abundant sterile ice was placed in the swine abdomen. After 4000 ml lavage, the liver was removed by sectioning the hilum and divided into lobes. Liver's segments were frozen at −80°C completely immersed in NaCl solution in sterile organ bags before decellularization.

3.3. Isolation and expansion of pMSC

BM aspirates (20-40 ml) were obtained from all animals under general anesthesia. Heparinized BM sample were collected from the posterior iliac crest using standard BM aspiration kits with a 15-gauge needle (Medax Mod Cage, Mantova, Italy) and immediately transported to the laboratory for processing.

Briefly, Mononuclear cells (MNCs) were isolated from BM by density gradient centrifugation on Lymphoprep (Ficoll 1.077 g/ml; Lymphoprep, Nycomed Pharma, Oslo, Norway). MNCs were plated on uncoated polystyrene culture flasks (Corning Costar, Celbio, Milan, Italy) at a density of 160,000/cm^2 in complete culture medium: DMEM-Low Glucose (Gibco Invitrogen, Paisley, UK) supplemented with gentamicin 50 mg/ml (Gibco Invitrogen) and 10% fetal calf serum (FCS Mesencult, Voden, Italy).

Cells were grown at 37°C in a humidified atmosphere containing 5% CO_2 and culture medium replaced twice a week. pMSCs were harvested, after reaching ≥ 80% confluence,

using Trypsin (Lonza, Milan, Italy), replated for expansion at a density of 4000 cells/cm^2 and propagated in culture until passage 4 (P4).

3.4. Characterization of pMSC

3.4.1. Proliferative capacity

The proliferative capacity of pMSC was defined as cumulative population doublings (cPD). The cPD was calculated by summing the PD of the single passage using the following formula:

$$PD = \log_{10}(N_1/N_0) / \log_{10}(2),$$

where N_0 is the number of cells seeded and N_1 the number of cells harvested at the end of the passage.

3.4.2. Immunophenotype

pMSC were phenotypically characterized by flow cytometry. Fluorescein isothiocyanate (FITC) or phycoerythrin (PE)-conjugated monoclonal antibodies specific for CD45, CD11b, CD90, CD105 and CD29 were used (BioLegend, San Diego, Calif). We included also appropriate isotype- matched controls (BioLegend).

In brief, cells were incubated with specific antibodies at the recommended concentrations for 30 minutes at 4°C. After that, the cells were washed with PBS supplemented with 0.1% BSA. Samples were centrifugated at 1000 rpm for 10 minutes and resuspended in 300 μl of PBS.

Data acquisition and analysis of cellular populations were performed by direct immunofluorescence with FACS Navios cytometer (Beckman Coulter).

3.4.3. Differentiative capacity

Cells were tested for their ability to differentiate into osteoblasts and adipocytes at early passages (P3). Briefly, to induce osteogenic differentiation, cells were cultured in specific differentiation medium: αMEM (Lonza, Veuviers, Belgium) supplemented with 10% FCS (Euroclone, Milano, Italy), dexamethasone (10^{-7} M), and ascorbic acid (50 g/mL). Starting from day +7 of differentiation culture, β-glycerolphosphate (5 mM, Sigma-Aldrich, Milan, Italy) was added. For adipogenic differentiation, cells were cultured in αMEM, 10% FCS and 2mM L-glutamine supplemented with 10^{-7}M dexamethasone, 50 mg/mL L-ascorbic acid, 100 mg/mL insulin, 50 mM isobutyl methylxanthine, 0.5 mM indomethacin (Sigma-Aldrich), and 5mM β-glycerol phosphate. Both osteogenic and adipogenic cultures were incubated for two weeks before evaluating differentiation at 37°C with 5% CO_2; media were replaced twice per week.

In order to detect osteogenic differentiation, cells were stained for alkaline phosphatase (AP) activity using Fast Blue (Sigma-Aldrich) and for calcium deposition with Alizarin Red S (Sigma-Aldrich). Adipogenic differentiation was assessed based on the morphological appearance of fat droplets after staining with Oil Red O (Sigma-Aldrich).

3.5. Liver decellularization procedure

The frozen liver segment was thawed in NaCl solution at room temperature for 24 hours. Subsequently, the liver lobe was cut into smaller segments (dimension of about 1x1 cm and 2 mm thick). Sample decellularization was obtained through a multistep procedure. First, liver samples (n=24) were put in continuous agitation on an orbital shaker at 50 rpm in 500 ml NaCl solution containing Heparin (5000 UI/ml, ….) for 12 hours. Second, liver samples were maintained in agitation on orbital shaker at 50 rpm in deionized H_2O (dH_2O) containing 0.15% Sodium Dodecyl Sulphate (SDS, Sigma-Aldrich) for 48 hours, in this step the solution being changed each 12 hours. Finally, when the decellularization was completed, the detergent must be removed from the specimens. Therefore, 6 wash with NaCl solution supplemented with antibiotic and antimycotic (1% amoxicillin/clavulanic

acid and 1% fluconazole) was performed. The rinse solution was changed each 12 hours. Then, after 72 hours, liver scaffolds were stored in the antibiotic and antimycotic solution at 4°C until cell seeding.

Every step has been carried out under a laminar flow hood and in complete sterile conditions.

3.6. Evaluation of decellularization

3.6.1. Hematoxylin eosin (H&E) staining

The histology tissue preparation included the following steps: fixation, dehydration, inclusion, microtomy, assembly and staining.

For H&E examination, 4% Paraformaldehyde (PFA) in PBS was prepared as fixative solution. Samples were fixed in 4% PFA for 24 hours at room temperature, rinsed twice with PBS solution, dehydrated with a gradient alcohol series, cleared in xylene and embedded in paraffin. ECM-sections (8 μm) were obtained using a Leitz microtome and prepared for histology.

In order to visualize the presence of residual nuclei and to assess the ultrastructure of the ECM, sections were stained with H&E and examined under a light microscope (Axiophot Zeiss, Oberkochen, Germany) equipped with a digital camera.

3.6.2. DAPI staining

Nuclear- specific 4,6-diamidino-2-phenylindole (DAPI) staining was performed to confirm the degree of cell removal.

ECM-samples were rinsed in PBS and fixed with 4% PFA for 30 minutes. After incubation, samples were washed 3 times with PBS. DAPI solution were dropped on each sample and incubated at room temperature for 10 minutes. ECM-sample marked with DAPI were observed at Confocal Microscope (Leica, Germany).

3.6.3. DNA extraction

DNA content was quantified using phenol/chloroform manual extraction methods. In brief, dry decellularized scaffolds (n=4) were weighed on analytic balance. Scaffold were then digested using 500 µl TNE buffer (Tris 10 mM, NaCl 150 mM and EDTA 10 mM) containing 30 µl of Proteinase K (10 mg/mL, Invitrogen) and 30 µl of SDS solution (20%). After 4 hours at 56°C incubation, 500 µl of Phenol solution (TNE saturated) were added to each sample. Samples were centrifugated at 8000 rpm for 5 minutes. The aqueous top layer containing DNA was recovered and then an equal amount of phenol-chloroform solution (1:1) was added. Samples were centrifugated at 8000 rpm for 5 minutes and the aqueous top layer was recovered. Phenol-chloroform-isoamyl alcohol (25:24:1; Acros) was added in equal amounts to each sample and centrifuged at 8000 rpm for 5 minutes. Ethanol was then added, and the solution kept at 4°C for at least 12 hours to allow DNA precipitation. After that, samples were centrifugated at 13000 rpm for 10 minutes to remove ethanol. Finally, DNA-free dH_2O was added to each sample. The total amount of DNA was quantified spectrophotometrically using NanoDrop (Thermo Scientific, Waltham, MA, USA).

In order to evaluate the DNA content in native liver, we applied the same DNA extraction procedure to fresh liver (n=3) after tissue dissociation by GentleMACS Dissociator (Miltenyi Biotec, Germany) following manufactory instructions.

3.6.4. SEM analysis

The bare scaffolds were washed twice with Sodium Cacodylate Buffer (SCB; 0.1 M, pH 7.4) for 7 minutes. Scaffolds were fixed with 2,5 % glutaraldehyde (GDA) and 2% PFA in SCB and then, incubated for 30 minutes at 37 °C. After fixation step, ECM-scaffold were rinsed twice with SCB for 7 minutes at 37 °C. Dehydration phase was carried out with ethanol at increasing concentrations (30%, 50%, 70%, 90% and 100% v/v), for 7 minutes at 4°C. Samples were left under laminar flow hood to completely dry for at least 12 hours, in order to eliminate solvents and samples were kept at 4°C until scanning electron

microscope (SEM) analysis. Finally, the dehydrated samples were platinum sputtered and high vacuum analysed by SEM (Mira3, TESCAN, Roma).

3.7. MSC seeding on ECM-scaffold

Prior to *in vitro* static culture, ECM-scaffolds were placed in a 48 well plate and incubated overnight in complete medium (D-MEM supplemented with 10% Mesencult, 0,1% gentamicin) at 37°C humidified atmosphere and 5% CO_2.

pMSC (1×10^6/50 µl) were seeded drop by drop on the liver ECM and incubated at 37°C and 5% CO_2 for 30 minutes. 1ml of complete medium was then added. The medium was changed twice a week. pMSC cultured on ECM-scaffold were evaluated after 3, 7, 14 and 21 days of in vitro static culture.

3.8. Evaluation of recellularization

3.8.1. Histological evaluation

In order to evaluate the ability of pMSC to growth on ECM, seeded ECM-scaffolds were evaluated for each timepoint by H&E staining, DAPI staining and SEM analysis following the procedures described above.

3.8.2. MTT Assay

Cell viability on recellularized scaffold was determined by 1-(4,5-Dimethylthiazol-2-yl)-3,5-diphenylformazan (MTT) assay (Sigma-Aldrich). With the same seeding protocol described above, 125.000 pMSC/50 µl were seeded drop by drop on the liver ECM. After 3,7,14 and 21 days, the culture medium was removed, and after a rinse with PBS, 500 µL of MTT solution (5 mg/mL in DMEM-Low Glucose) were added on each well containing the scaffold and incubated for 4 hours at 37 °C to allow MTT reduction by viable cell mitochondrial dehydrogenase. Supernatants were removed from the wells, and 500 µl of 0.1% HCl in isopropanol were added to dissolve blue formazan crystals inside the cells

giving a blue solution. Optical density (OD) of solution was measured at 570 nm by ELISA Microplate Reader (Microplate Reader Model 680, Sunrise). The colour intensity is proportional to the number of viable cells. Number of cells (media ± SE) are extrapolated from a standard curve obtained with defined number of pMSCs (Fig.5).
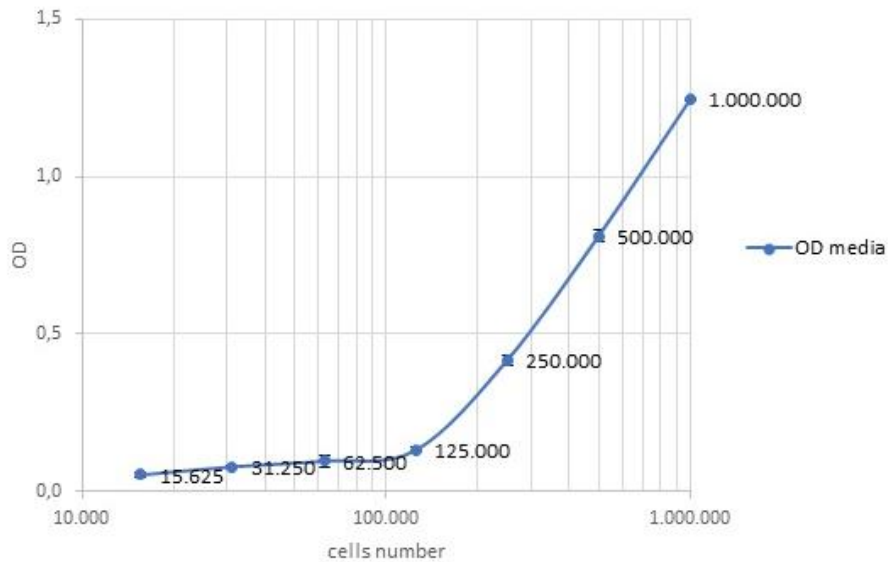
Number of cells	15.625	31.250	62.500	125.000	250.000	500.000	1.000.000
OD media	0,0538	0,0810	0,0978	0,1320	0,4175	0,8120	1,2450
SE	0,0069	0,0026	0,0200	0,0075	0,0160	0,020	0,0012

Figure 5: Standard curve for MTT assay. The standard curve is obtained through serial dilutions of pMSC samples at defined concentration and show the absorbance of different concentrations of cells. Six replicates for each concentration were performed and data were expressed as OD mean ± standard error (SE). The cell concentration of the unknown sample may be calculated by interpolation on the graph.

3.8.3. PAS staining

To detect glycogen synthesis, cells were stained using Periodic acid Schiff (PAS) staining kit (Bio-optica). Cells cultured on scaffold at each timepoint were fixed in 4% PFA. ECM-sections (8 µm) were washed with distilled water. 10 drops of PAS solution (reagent A) were put on the section and leaved to act 10 minutes. After incubation, sections were rinsed in distilled water. 10 drops of Schiff reagent Hotchkiss McManus (reagent B) were put on samples and leave to act 20 minutes.

Sections were wash with distilled water. After that, Potassium metabisulphite solution (reagent C) were dropped on the section and leaved to act 2 minutes. Without washing, the fixative solution (reagent D) was added and leaved to act 2 minutes.

After a rinse in distilled water, the sections were staining with Mayer's Hemalum (reagent E), incubated for 3 minutes and then washed in running tap water for 5 minutes. Finally, sections were dehydrated through ascending alcohols and cleared in xylene.

Samples were examined under a light microscope (Axiophot Zeiss, Oberkochen, Germany) equipped with a digital camera.

3.9. Gene expression

3.9.1. RNA extraction

At each time point, total RNA from seeded scaffold was extracted using the acid guanidinium thiocyanate-phenol-chloroform method. Cells on scaffold were lysed by adding 1 ml of PureZOL (Bio-rad). To improve the efficiency of the cell lysis process, the lysate was passed through a 28-gauge needle and syringed several times. The lysate was incubated at room temperature for 5 minutes, to allow the complete dissociation of nucleoprotein complexes. After incubation, 0.2 ml of chloroform was added. Samples were centrifugated at 12.000 rpm for 15 minutes at 4°C and the aqueous top layer containing RNA was recovered. Subsequently, 0.5 ml of isopropyl alcohol was added. Samples were centrifugated at 12.000 rpm for 15 minutes at 4°C. After discard the supernatant, RNA pellet was washed with 1 ml of 75% ethanol. Samples were vortexed and then centrifugated at 7.500 rpm for 5 minutes at 4°C to remove ethanol. After discard the supernatant, RNA pellet was resuspended in 20 μl of nuclease free water (nuclease free- H_2O).

Extracted RNA was tested for quantity and integrity by spectrophotometric analysis (NanoDrop).

RNA sample extracted from fresh liver was used as positive control.

3.9.2. Retrotrascription

A total of 1 µg of RNA per condition was reverse transcribed into complementary DNA (cDNA) using Reverse Trascritional M-MLV RT kit (Promega). 1 µl of Oligo (dt) primers was added on each sample and incubated for 5 minutes at 70°C. PCR solution containing a mixture of deoxynucleotides (dNTPs, Roche), Recombinant Rnasin Ribonuclease Inhibitor, M-MLV RT, reaction buffer and nuclease free H_2O was prepared and 20 µl added to RNA sample. Samples were incubated for 1 hour at 37°C and then for 10 minutes at 65°C.

cDNA was analysed for quantity and integrity spectrophotometrically using NanoDrop.

3.9.3. Real-Time PCR

Real-time PCR for albumin (ALB), alpha fetoprotein (AFP), cytochrome 450 subfamily 1a (Cyp1a), cytochrome 450 subfamily 7a (Cyp7a), cytokeratin 18 (Krt18), hepatocyte nuclear factor 4a (HNF4a) were evaluated.

The assay master mix containing iTaq Universal Probes Supermix 2x (Bio-Rad), primer and fluorogenic probes for each gene tested were prepared. Equal aliquots of assay master mix were dispensed into the wells of MicroAmp Optical 96-Well Reaction Plate (Applied Biosystems).

100 ng of cDNA per condition were added into each well containing the reaction setup. The plate was covered with a MicroAmp Optical Adhesive Film and spinned for 30 seconds to remove any air bubbles and mix the reaction components.

The thermal cycling protocol was programmed on the Real-Time PCR instrument (AB 7500 Standard System) following the instructions:

- Polymerase Activation and cDNA denaturation: 30 seconds at 95°C
- 40 amplification cycles composed of:
   - Denaturation: 15 seconds at 95°C
   - Annealing/Extension: 60 seconds at 60°C.

Data analysis were performed by 7500 fast Real-time PCR systems (Applied Biosystems). The glyceraldehyde 3 phosphate dehydrogenase (GADPH) was used as endogenous

internal control. The relative quantification (RQ) of the genes of interest in relation to the housekeeping gene (endogenous reference gene) was calculated on the basis of the "delta delta Ct" (ΔΔCt) method, and the result were expressed as RQ.

Normalization was carried out by applying the following formula:

$$\text{Fold expression} = 2^{-\Delta\Delta Ct}$$

where 2 represents the amplification efficiency of 100%, and

$$\Delta Ct = Ct \text{ reference gene} - Ct \text{ gene of interest.}$$

$$\Delta\Delta CT = \Delta CT \text{ seeded scaffold} - \Delta CT \text{ control}$$

3.10. Statistical analysis

Comparison of DNA quantification between native liver and ECM-scaffold was performed by Two-sample Wilcoxon rank-sum (Mann-Whitney) test. p value ≤ 0.05 was considered significant.

4. RESULTS

4.1. Liver decellularization.

Porcine livers were successfully obtained using a surgical technique similar to the one used for multi-organ explant in a human cadaveric donor. After organ explantation, livers were kept frozen until decellularization.
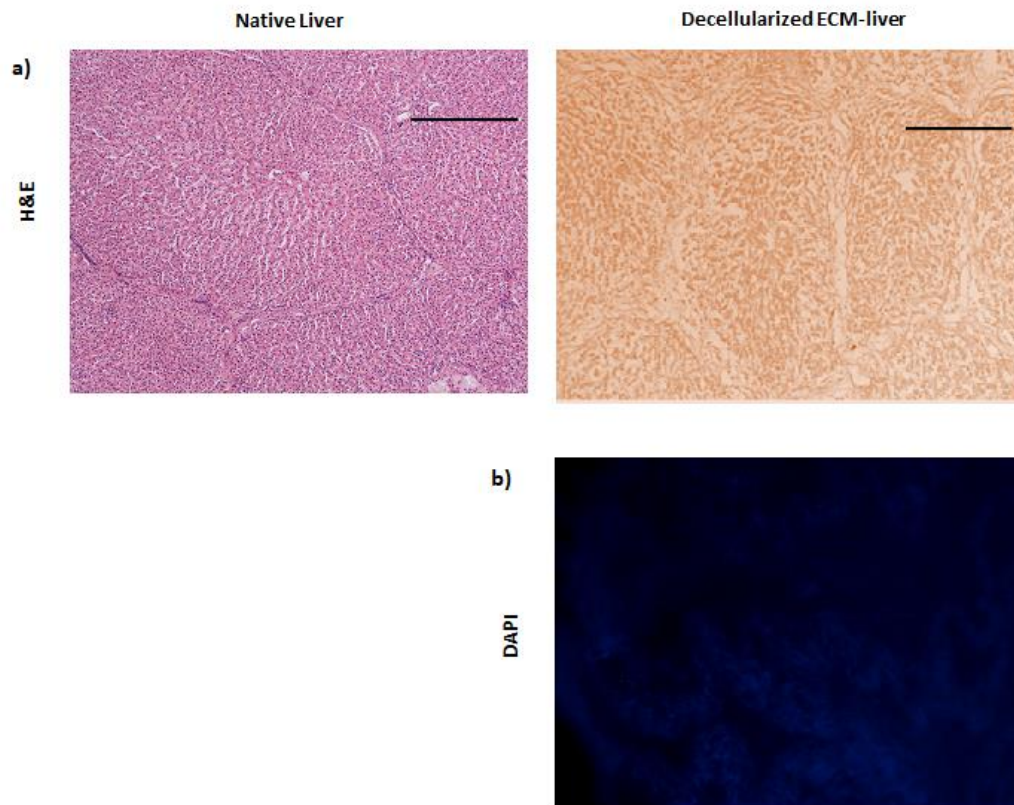
During the decellularization procedure, the macroscopic appearance of the liver specimens changed, from dark red to white/translucent confirming the detachment of the cells from the ECM scaffold (Fig. 6).
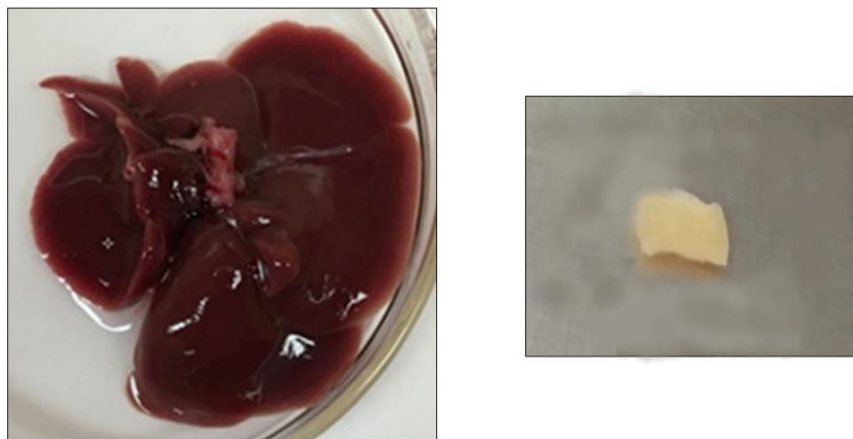
Figure 6: Macroscopic appearance of porcine liver before and after decellularization procedure. The liver was removed from the -80°C freezer and maintained at room temperature for 24 hours. A single lobe was then cut into small cube of approximately 1cm³. After SDS treatment, ECM-scaffolds reached white transparency and did not present any areas of tissue remaining in the scaffold.

The efficacy of the decellularization protocol was confirmed both qualitatively, by H&E and DAPI staining and quantitatively by DNA extraction.

H&E staining is one of the principal tissue staining used in histology. H&E staining showed the absence of cell nuclei on ECM and the preservation of the integrity of extracellular matrix after decellularization procedure. Moreover, in order to confirm the degree of cell removal, DAPI staining was performed. As reported in Fig. 7, we showed the absence of cells on the ECM.

Figure 7: *Efficacy of the decellularization protocol confirmed qualitatively, by H&E and DAPI staining. Panel a: H&E staining before and after decellularization procedure. The haematoxylin stains in blue or dark purple cell nuclei, and eosin stains in pink cytoplasm and other structures including extracellular matrix. On the left, H&E staining in a section of pig liver. H&E stained images display nuclei (blue/dark purple) and tissue components (pink). On the right, blue or dark purple nuclei are no longer detected with HE following decellularization procedure and the preservation of ECM integrity is highlighted by eosin. Panel b: DAPI staining of liver matrix after decellularization with SDS. absence of fluorescent nuclei on ECM-scaffold. DAPI is a fluorescent stain of cell nuclei, since binds strongly to adenine–thymine rich regions in DNA.*

Finally, the quantification of the decellularized scaffold displayed levels of DNA residues compatible with standard criteria of optimal decellularization, being lower than 50 ng of double-strand DNA (dsDNA) per mg of dry weight of scaffold (Fig. 8). In fact, the average quantification obtained of residual DNA from a decellularized scaffold was $20 \pm 2,4$ ng/mg dry weight (mean $\pm$ SE). Furthermore, we demonstrated that residual DNA in decellularized scaffold was lesser than 3,5% of the amount of DNA obtain to equal size of fresh liver.
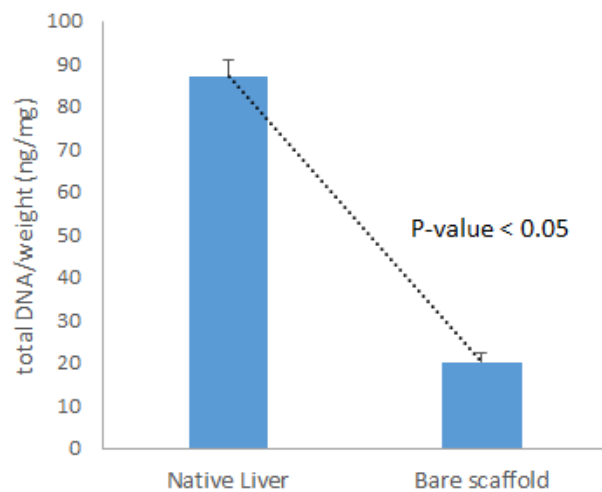
Figure 8: *Level of DNA extracted from native liver and dry weight ECM-liver scaffold. Decellularization process efficiently remove DNA content of liver ECM. Data are shown as mean ± SE. Total DNA quantification demonstrated significant DNA reduction from 59266,2 ng in native liver to 2069,6 ng in bare scaffold. DNA reduction are statistically significative (p value < 0.05). The percentage of residual DNA was lesser than 3,5% of the DNA present in fresh tissue.*

4.2. 3D architecture and ultrastructure.

The integrity of 3D microanatomy and ultrastructure of extracellular matrix after decellularization was investigated by SEM analyses (Fig. 9).

SEM imaging revealed the maintenance of key hepatic features including the honeycomb-like arrangement and the presence of an organized network of ECM fibrils associated with liver lobules. In addition, portal tracts were preserved after decellularization as well as the size of cellular pockets within the parenchymal space which was in the region of 15–30 μm corresponding to the approximate size of a hepatocyte.

Overall, these data confirm the preservation of the micro and nano architecture of ECM-scaffold following decellularization.
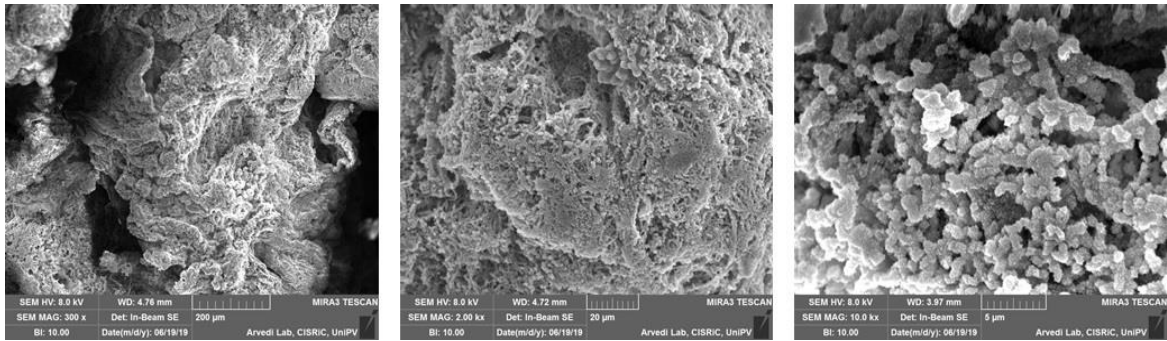
Figure 9: SEM imaging of decellularized scaffold at different magnification (300x, 2kx and 10kx respectively). Scanning electron microscopy analysis of the ECM showed rough surface in absence of cells and preserved three-dimensional structures characterized by high interconnected porosity.

4.3. Mesenchymal Stromal Cells isolation and characterization

Porcine MSC (pMSC) were successfully isolated and expanded in vitro from all porcine BM samples, reaching at P4 (early passage) a total number of cells that allowed experimental applications. After isolation and expansion, pMSCs were characterized for their morphology, immunophenotype, proliferative, and differentiation capacities, in order to evaluate their correspondence to the minimal criteria for mesenchymal stem cells definition [147].

Cells were plastic adherent and showed the typical spindle-shaped morphology in *in vitro* culture (Fig. 10a). They displayed a normal growth capacity evaluated in terms of cPD, from P1 to P4 (Fig. 10b). The expression of pMSCs surface markers, evaluated by flow cytometry, showed that ≥ 95% of cells were positive for CD90, CD29, CD105, and ≤ 5% negative for CD45 and CD11b (Fig. 10c).
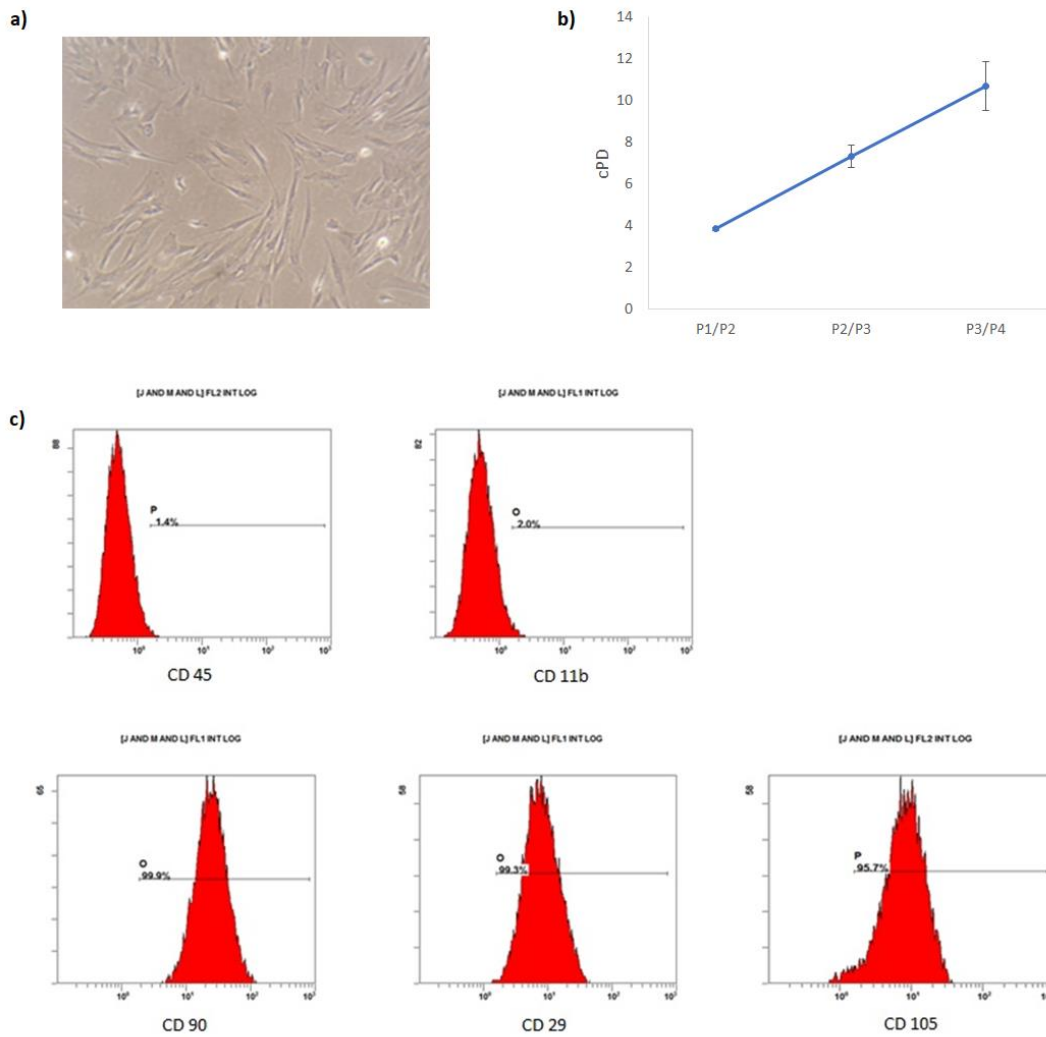
Figure 10: *Porcine BM-MSCs characterization. Panel a: pMSCs display the characteristic spindle-shaped morphology (magnification 4x); Panel b: cumulative population doubling (cPD) from P1 to P4 of pMSCs. The data represent the mean ± SD of all BM samples processed (n=3); Panel c: immunophenotype: pMSCs are characterized by the expression of the typical surface markers: CD90, CD29, CD105 and the absence of typical hematopoietic cell markers: CD45 and CD11b.*

Moreover, we showed that pMSC, upon specific *in vitro* conditions, were able to differentiate toward adipogenic and osteogenic lineages In particular, pMSC differentiated into osteoblasts, as demonstrated by the histological detection of calcium depositions positive for Alizarin Red and by the activity of Alkaline phosphatase, and into adipocytes, as shown by the morphological appearance of lipid droplets stained with Oil Red O. (Fig. 11).
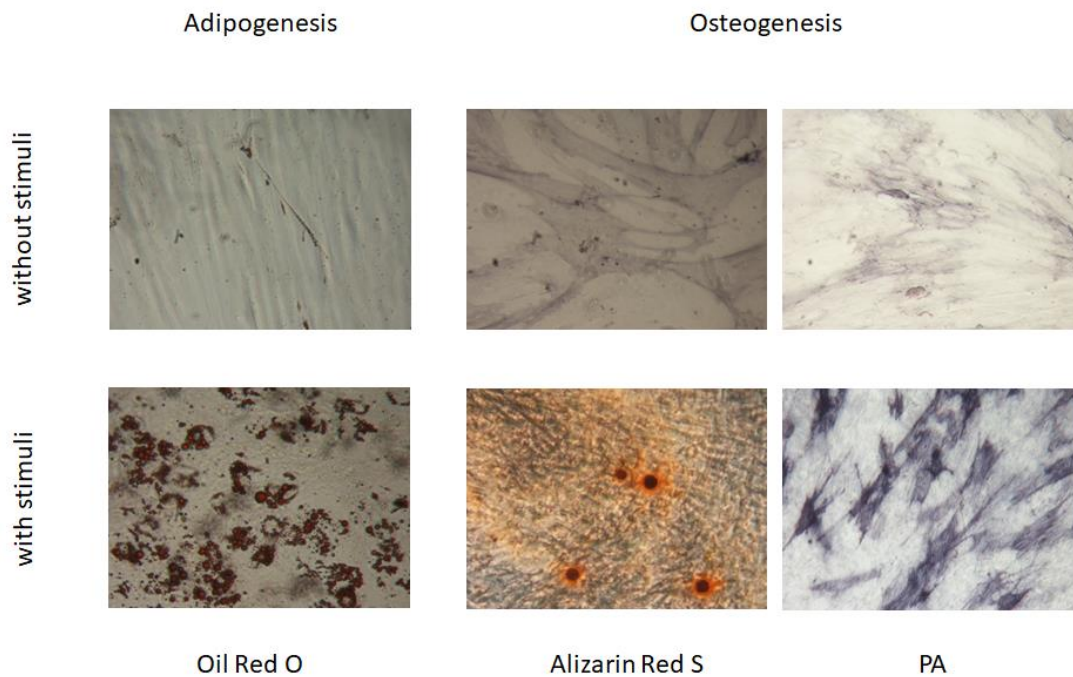
Figure 11: *Differentiation ability of pMSC in adipocytes and osteoblasts. The differentiation into adipocytes is revealed by the formation of lipid droplets stained with oil red O. The differentiation into osteoblasts is demonstrated by the histological detection of calcium depositions positive for Alizarin Red S and by the histological detection of alkaline phosphatase activity (PA). Original magnification 20x for adipocyte staining and 10x for osteoblast staining.*

Our results confirmed that the cells isolated from porcine BM, following human MSC isolation standard procedure, were phenotypically and functionally mesenchymal stromal cells, suitable to be used for liver ECM recellularization.

4.4. H&E staining after recellularization

In order to evaluate pMSCs adhesion and proliferation on ECM, seeded scaffolds at 3, 7, 14, 21 days of culture were fixed, stained with H&E and evaluated by optical microscopy. As shown in Fig.12, we can demonstrate the capacity of pMSCs to adhere and grow on ECM, in fact, the cells number on scaffold surface increased progressively over the culture time.

Moreover, in order to verify the ability of cells to infiltrate inside the structure of the ECM and colonize the inner layers, each scaffold was cut at different depths. Sections have been evaluated after staining with HE. We observed that also the number of cells in the inner layers increased with increasing days of culture, showing that pMSCs can repopulate the matrix growing not only on the surface but also at deeper levels.

Bare scaffold

3 days　　　　　　**7 days**

14 days　　　　　**21 days**
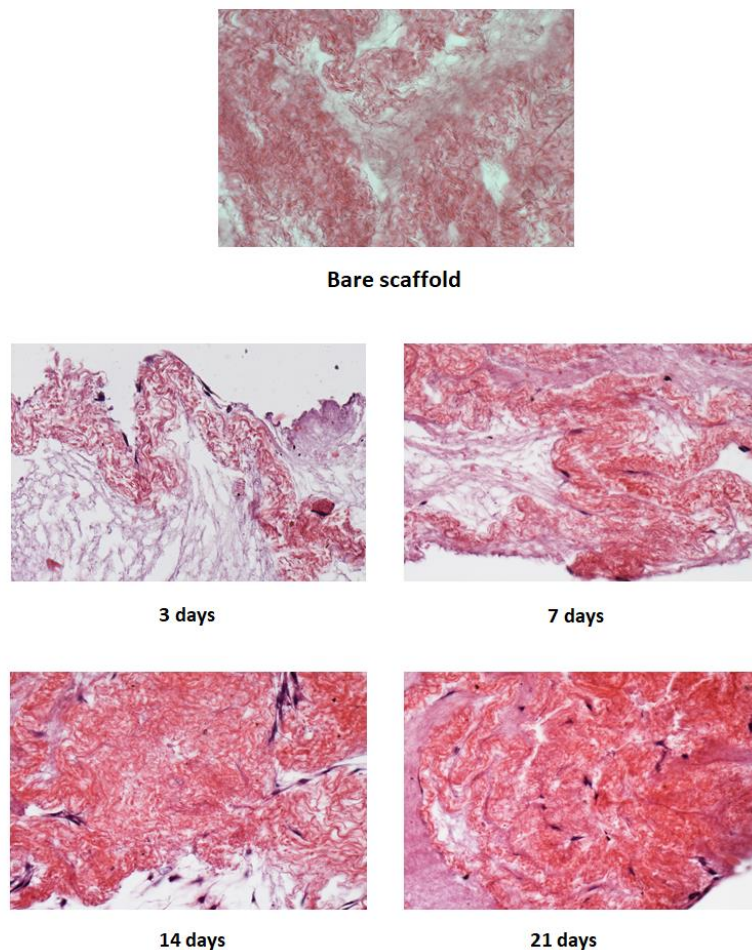
Figure 12: *HE staining after recellularization. Cells nuclei stained in blue and cytoplasm and ECM stained in pink are shown in the 4 different timepoints. (Original magnification 20 x).*

4.5. DAPI staining after recellularization

At each timepoint, the scaffold repopulation was evaluated also by fluorescence microscopy, using DAPI staining. As shown in Fig. 13, despite the ECM auto-fluorescence, that slightly interfered with imaging, it was possible to evidence stained nuclei of cells on

the ECM surface. Therefore, also with this approach we clearly demonstrated that with increasing of the culture days, the number of adherent cells enhance progressively, reaching almost a complete scaffold coverage.
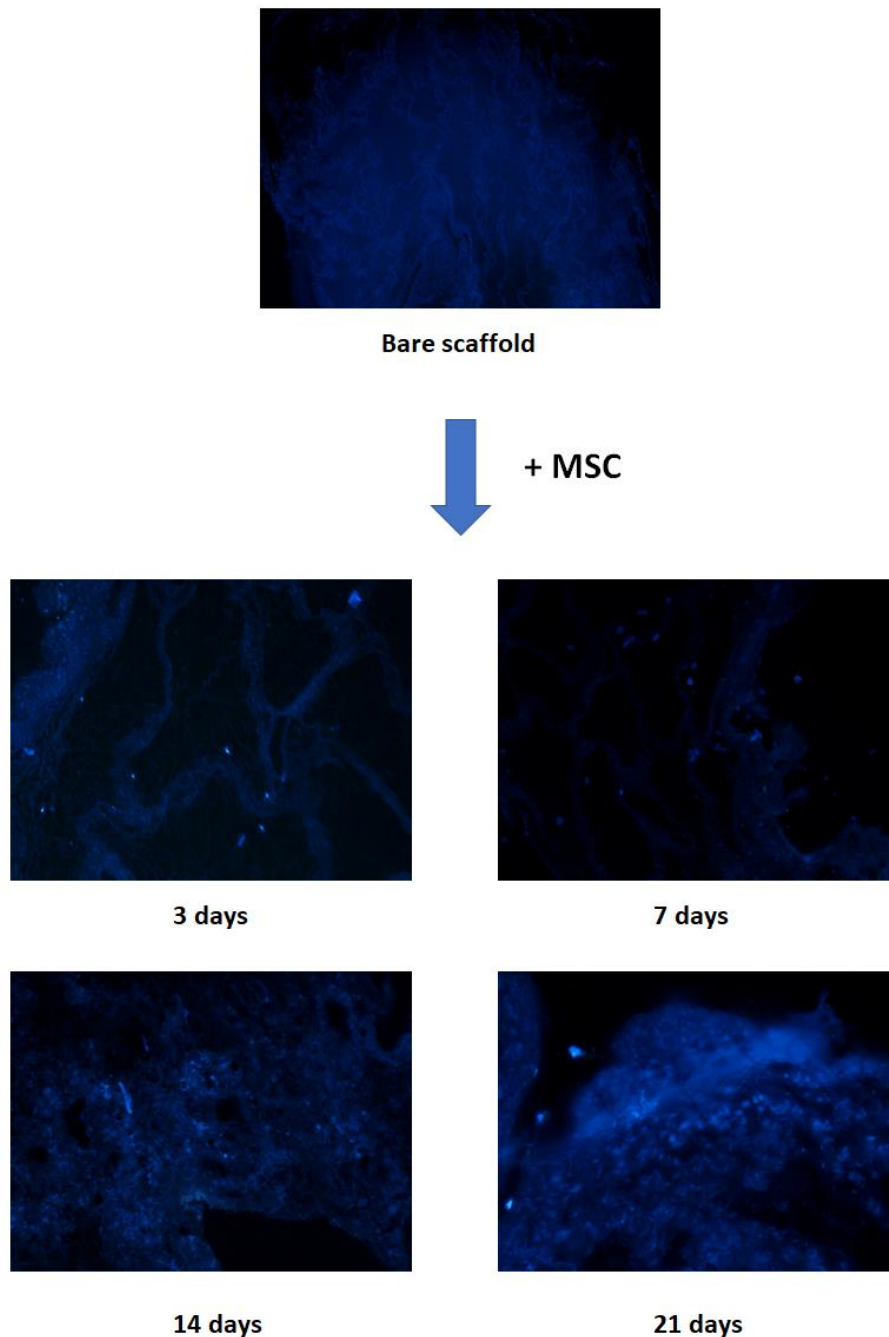
Figure 13: DAPI staining after recellularization: Cells nuclei stained in blue are shown at the different timepoints. (Original magnification 40x). DAPI emits blue fluorescence upon binding to AT regions of DNA. Nuclei staining with DAPI appear as brilliant spots. The scaffold surface covered by cells increases progressively with increasing culture time.

4.6. SEM recellularization

We performed SEM analysis on recellularized scaffolds at 3, 7, 14 and 21 days to confirm the presence of p-MSCs and their degree of repopulation (Fig. 14). At each timepoint, the cells seem to be well attached to ECM scaffold. We find a progressive increase of cells number over the culture days. By SEM analysis we could highlight the capacity of these cells to form colonies that progressively enhance in size.

Furthermore, no signs of cell suffering as morphological alteration or cell detachment are evaluated at 21 days, suggesting that ECM scaffold may represent a good microenvironment for cell survival. In some images, we also could observe that cells started to form intracellular junctions and to develop new extracellular matrix, representing a positive step for the recellularization.
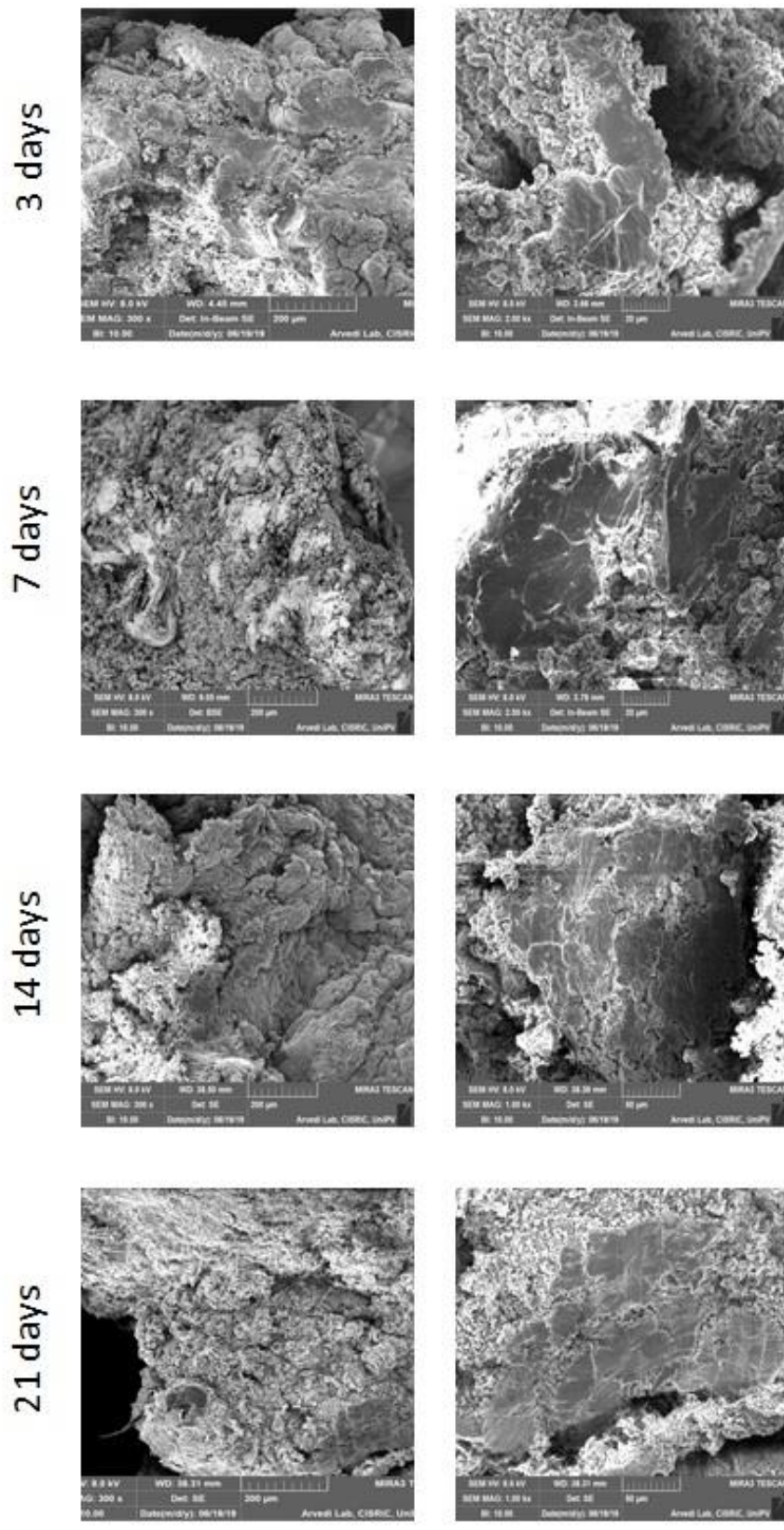
Figure 14: *SEM analysis at each timepoint of recellularization at different magnification (from 300x to 2kx). The capacity of these cells to form colonies progressively enhance in size.*

4.7. Cell Viability determination

At 3, 7, 14, 21 days of culture, the viability of pMSCs on ECM-scaffold were tested. Only viable cells with active metabolism can convert MTT into formazan crystal by cell mitochondrial dehydrogenase activity and the intensity of blue/purple product are proportional to the number of cells.

With this approach, we created a standard curve with defined number of pMSCs in order to obtain a quantification of recellularization.

We could observe that cells on scaffold were increased progressively to the culture days. Number of cells are extrapolated from standard curve and reported as media ± SE. On average, quantification showed that cells grown on scaffold increase by 5,5-fold at days 21 of culture (Fig. 15).
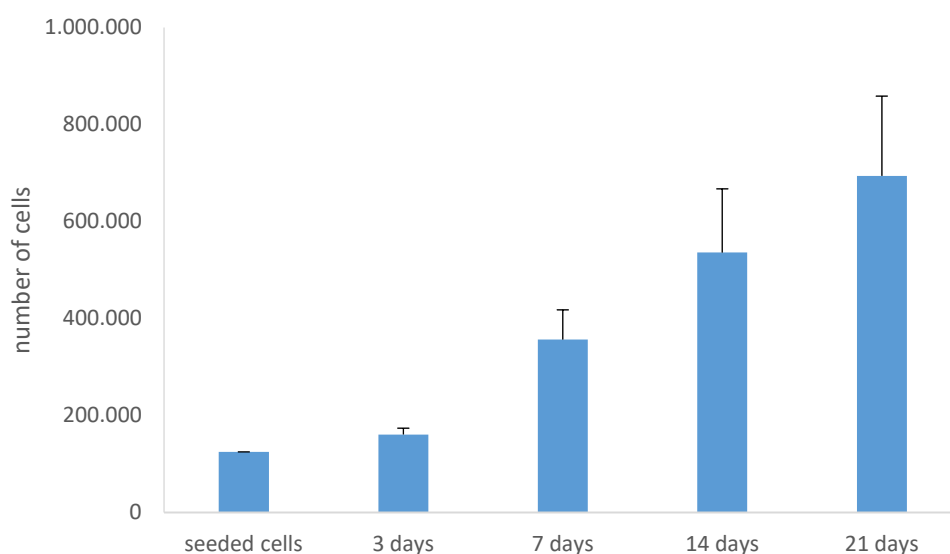
Figure 15: *Number of viable cells at each time point assessed by MTT assay. Results are reported as mean of 4 replicates ± SE.*

4.8. PAS staining

In order to evaluate the ability of pMSCs seeded on ECM to store glycogen, scaffolds at 3, 7, 14, 21 days of culture were fixed, stained with PAS and evaluated by optical microscopy.

We observed that also the number of cells in the inner layers increased with increasing days of culture, showing that pMSCs are present in each time point considered (Fig.16). However, no signs of PAS positivity are evaluated after 3D culture.

Bare scaffold

3 days

7 days

14 days

21 days
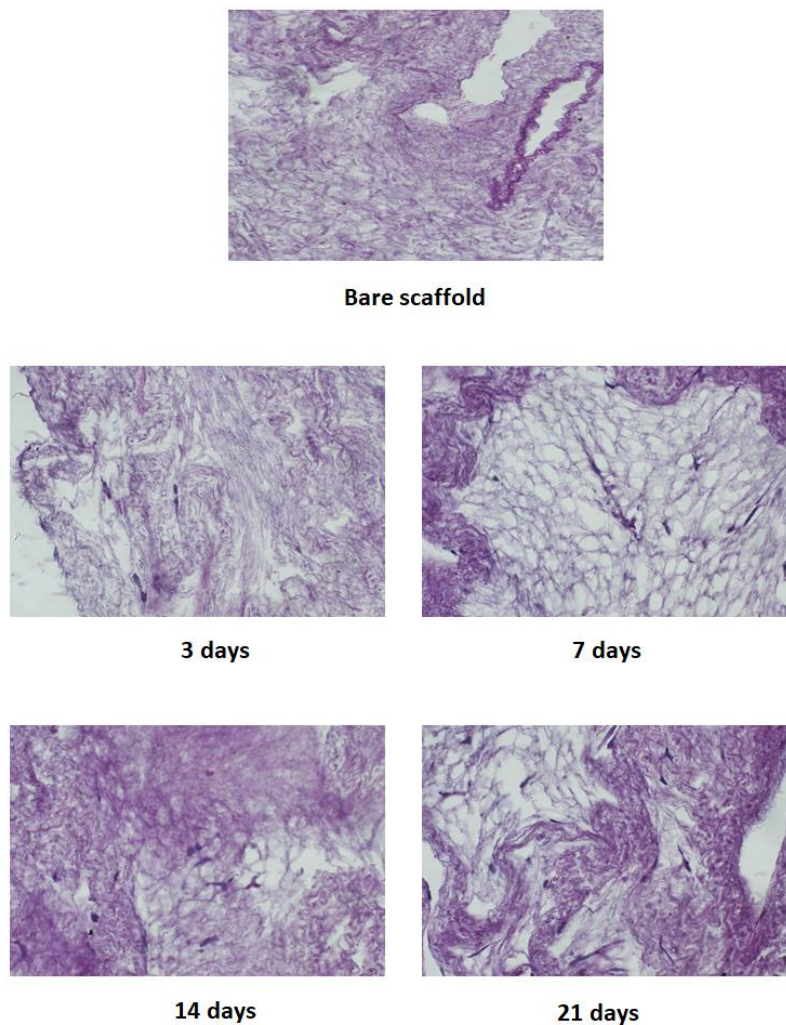
Figure 16: *PAS staining. PAS stained cells in dark purple and polysaccharides such as glycogen in pink/red. No deposits of glycogen are shown in the 4 different timepoints. (Original magnification 40x).*

4.9. Gene expression

RNA was successfully extracted from all ECM samples and retrotrascripted in cDNA. In order to determinate whether culture on liver ECM-scaffold could promote/address differentiation of pMSC towards hepatocyte, the transcriptional levels of some hepatic genes were tested. In particular, we evaluated six genes associated to different phases of the hepatic development. A comparison with the expression profile was made with both porcine primary hepatocyte and pMSC. We used as calibrator the hepatocyte.

For Krt18, ALF, HNF4a, and CYP1a1 genes the relative expression levels of seeded pMSC did not differ to native pMSC one. While no expression of albumin (ALB), the typical marker of hepatocyte functionality, was observed at any timepoint, CYP7a1 gene was expressed by hepatocytes, and by seeded pMSC, but not by native pMSC (Fig. 17). These data could support the hypothesis that the interaction with liver ECM may induce a differentiation toward hepatic progenitors, but it is not enough to induce the complete maturation in functional hepatic cells RNA was successfully extracted from all ECM samples.
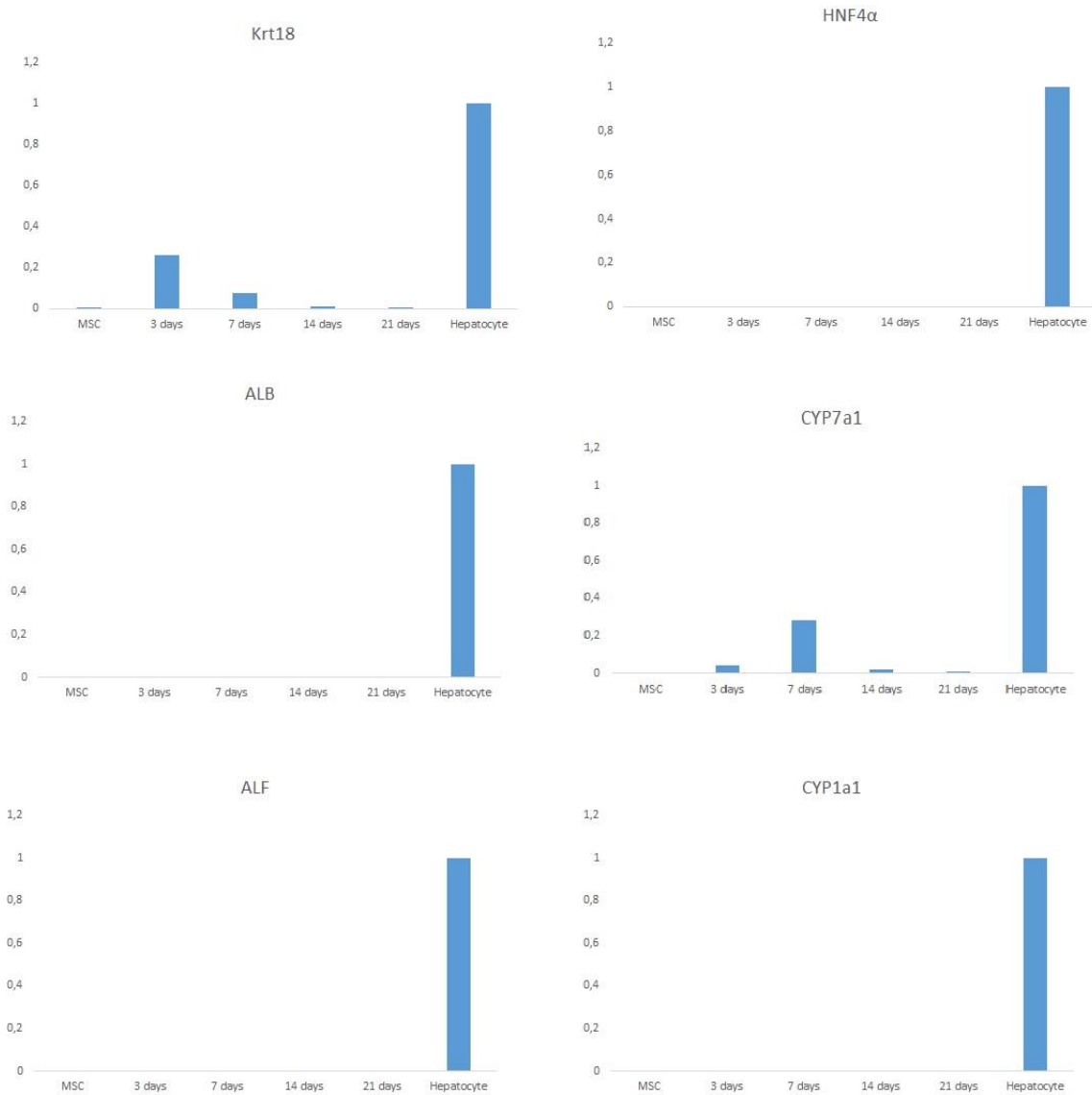
Figure 17: *RT-PCR analysis for six hepatic-specific genes. Thanks to molecular analysis, it was possible to evaluate the expression of mRNA coding for proteins involved in hepatocyte differentiation, such as Krt18, HNF4a, ALB, CYP7a1, ALF and CYP1a1. Results are expressed as RQ, normalizing the expression of gene of interest, with the expression of a reference gene (GAPDH) in the same sample.*

5. DISCUSSION

One of the most difficult challenge for organ bioengineering is to recreate functional organs for clinical applications. The hope is to find a way to overcome both the shortage of organs and the need to immunosuppressive treatment, representing the limits of the liver transplant. In this context, towards the clinical translation, one of the most important issue to get over is to obtain a clinically relevant sized hepatic scaffold to repopulate. For liver bioengineering, porcine livers are an optimal source of organs for decellularization. In fact, porcine livers are very close for size to human counterpart, becoming a good acellular and non-immunogenic three-dimensional surface able to be repopulated with human cells to satisfy the clinical request.

Within ECM-scaffold base technology, there are three main phases in the preclinical setting to take into account: the organ decellularization, the recellularization process and the cell signalling influenced by the interactions between cells and extracellular matrix (ECM).

In this study, we evaluated the feasibility to repopulate with porcine MSC (pMSC) the extracellular matrix obtained through porcine liver decellularization, and the possible ECM influence in promoting differentiation of pMSC towards hepatocyte.

As this purpose, the first part of the study was focused on the creation of porcine liver scaffolds. For this intent, we optimized an already standardized protocol used in our group for kidney decellularization. The organs were successfully obtained from four piglets following the standard procedure used for multi-organ explant in human donors. A tri-step of decellularization protocol was used. The liver was removed from the piglet and then carefully washed to completely remove blood from the vessels and to avoid clots formation. Then, liver lobes were accurately separated and maintained in sterile organ bags at -80°C until decellularization. The organ freezing can be considered the first step of our decellularization protocol. It was well demonstrated that the freeze/thaw cycles represent one of the physical methods used for decellularization [159]. In fact, the

freezing in the absence of cryoprotectants causes ice crystals formation within the cytoplasm that result in cellular membrane rupture. A single cycle of freezing/thawing could enhance the native cells detachment without damaging the structure of ECM. After freezing, the liver was thawed at room temperature for few hours and cut into small samples under sterile conditions.

These small pieces were subjected to the second step of decellularization, based on the use of SDS solution. SDS is a strong and harsh detergent that lyses cell membrane and causes interruption of noncovalent bonds between ECM structural proteins. SDS treatment was performed in agitation on an orbital shaker to enhance the effect of the treatment.

Finally, the third step of our protocol was necessary to remove the chemical residues and the cellular debris. In literature, it has been observed that SDS could interfere with the repopulation of ECM and produce serious toxic reactions once *in vivo* transplanted. In preliminary experiments, we could define that the concentration of SDS that allow cell growth is approximatively 1000 folds lower than that used for decellularization. For this reason, samples were rinsed several times.

Crapo et al. has described some of the minimal criteria to define a good decellularization process, underlining that evaluation of the residual materials within the decellularized scaffolds is mandatory [54]. In fact, evidences showed that cellular remnants lead to *in vitro* cytotoxicity and evoke *in vivo* adverse host responses. At this stage, arise the need to completely remove the cellular component from the ECM without using excessively aggressive methods in order to keep its three-dimensional structure. Therefore, the goodness of decellularization process can be evaluated by different approaches such as the absence of visible nuclear material in tissue sections, an amount of dsDNA extracted from decellularized scaffold lower than < 50 ng/mg of dry weight and residual DNA extracted fragment shorter than 200 bp.

In the present study, following the criteria of good decellularization process, we analysed the histological characteristics of ECM after decellularization. At first, the presence of nuclear material was qualitatively and quantitatively evaluated. On the decellularized

scaffold, no evidence of cellular nuclei was found and an intact cellular matrix without damage was observed.

DNA quantification of the decellularized scaffold displayed levels of DNA residues compatible with standard criteria of optimal decellularization. Moreover, our result showed that only 3,5% of the total DNA extracted from native liver, as present following our decellularization protocol.

By scanning electron microscopy, the decellularized scaffold appeared as a rough surface, with a preserved three-dimensional network of the vascular structures of the native organ. In some points it was also possible to observe some gaps compatible with a single hepatocyte dimension, that may represent a print left by the removal of native cells. Moreover, the preserved continuity of the ECM and the absence of alterations suggested that the decellularization protocol and the chosen solvent did not alter the ECM architecture.

For all these reasons, we considered that the combination of chemical and physical agents used in our protocol allowed to obtain a 3D structure adequate for the recellularization phase.

At this time, we proceeded to recellularization process using as cell source MSC isolated from porcine BM. MSC are considered good candidate for cell therapy for their ability to *in vitro* expand, reaching adequate cell number and maintaining specific functionalities. In literature, MSCs are describe as an optimal cellular source for scaffold repopulation in the field of solid organ transplantation. In particular, because of their ability to transdifferentiate into hepatocyte-like cells [123, 124, 160, 161], MSC may represent a good cellular source for liver regeneration. In our study, pMSC were successfully isolated and expanded *in vitro* from all porcine BM samples using the standard protocol for human MSC [163]. The characterization of pMSCs showed that these cells presented the typical morphology, proliferative capacity, immunophenotype and the ability to differentiate into osteoblasts and adipocytes [164].

A series of preliminary experiments have been carried out to define and standardize the re-seeding procedure, defining the optimal cell number, the type of seeding technique (static or dynamic) and the volume of cell suspension. During the recellularization

procedure, we observed that seeded cells slipped on scaffold surface and adhered to the well bottom. Therefore, it was decided to change the size of the scaffold to cover exactly the surface of the well.

Then, the ability of pMSCs to grow on ECM-scaffold was evaluated qualitatively and quantitatively at different time points.

A progressive increase of cell number on the scaffold surface was observed with increasing culture days, with a sustained infiltration of cells inside the scaffold at the 14th and 21st day.

3D images relating to various areas of the sample showed a flat, smooth and homogeneous surface covering the rough structure of the scaffold. After 14 and 21 days of culture, it was also possible to note the presence of large smooth surfaces representing more repopulated areas.

As describe above, MTT assay was used, by creating a standard curve, to evaluate quantitatively the degree of repopulation. Also, by this approach, we observed that the number of cells progressively increases at the different time points, confirming the presence of adherent and proliferating cells on the ECM scaffold. Therefore, it was concluded that pMSCs, and in general MSC, may represent a good cell population for recellularization of ECM scaffolds.

Recent studies in organ bioengineering have shown that preservation of ECM induces stem cells to differentiate into tissue-specific cells. Although the role of ECM in hepatic maturation of iPSCs was not fully understood, Park et al have showed that ECM liver in addition to specific growth factors may enhance liver cells development and maturation [82]. In another study, Lee et al demonstrated that the presence of rat extracellular matrix increased hepatics gene expression in hepatocyte like cells (HLCs) derived from human MSC [162].

In this regard, to determine whether porcine decellularized liver ECM could influence hepatic differentiation of pMSCs, we evaluated the expression of cell differentiation markers from seeded scaffold. Six genes (ALB, AFP, HNF4a, Cyp1a1, Cyp7a1 and Krt18) expressed at different time of hepatocyte development were considered. Of interest, we observed that Cyp7a1 gene, expressed in hepatocyte but not in MSC, was present in pMSC seeded scaffolds at each time points. Cyp7a1 is one isoform of the cytochrome

P450 superfamily of oxidative metabolism enzyme. In our opinion, these data support the hypothesis that the extracellular matrix can induce in pMSCs the acquisition of a hepatic progenitor phenotype.

6. CONCLUSIONS

The observations obtained so far allow us to state that:

• our decellularization protocol is effective in the removal of the cells from native liver, respecting the parameters for decellularization without damage the structure of ECM;

• porcine MSCs obtained from swine BM have characteristic comparable to those of their human counterparts and therefore they can be used as a model for experimental studies;

• the static seeding strategy of MSCs on the scaffold resulted to be effective in terms of ECM cell attachment, cell proliferation and migration inside the specimen.

• the genic profile of cells seeded on ECM scaffold without any growth factors is more similar to pMSC suggesting that the only contact with liver specific ECM is not strong enough to induce a complete differentiation in HLCs. Despite this, we observed an increase of a single gene activity (Cyp7a1) absent in pMSC.

To summarize, we can observe that our results are in accordance with data reported in literature and sustain the possibility to use decellularizated organs as biological scaffold to create functional organs.

To date, several studies on the extracellular matrix reveal that exists a state of dynamic reciprocity between cells and extracellular matrix. From now on, researches will therefore be focus on the necessity to reveal the complex and delicate dynamic equilibrium between cell and extracellular matrix, allowing the generation of new organs.

We believe that our results may provide new insights toward a better understanding of early HLCs development on ECM-scaffolds. However, a more detailed decellularization process, a better cell differentiation capacity and a more detailed understanding of the interaction between cells and ECM could represent crucial steps in the progression of this research field. For this purpose, several efforts will be necessary to understand preliminary data in order to make possible the translation to the clinical setting.

7. REFERENCES:

1. Sarin, S.K.; Choudhury, A. Acute-on-chronic liver failure: Terminology, mechanisms and management. Nat. Rev. Gastroenterol. Hepatol. 2016, 13, 131–49.

2. Bernal, W.; Auzinger, G.; Dhawan, A.; Wendon, J. Acute liver failure. Lancet 2010, 376, 190–201.

3. Boulter, L.; Lu, W.Y.; Forbes, S.J. Differentiation of progenitors in the liver: A matter of local choice. J. Clin. Invest. 2013, 123, 1867–1873.

4. Briceno, J.; Padillo, J.; Rufián, S.; Solórzano, G.; Pera, C. Assignment of steatotic livers by the mayo model for end-stage liver disease. Transpl. Int. 2005, 18, 577–583.

5. Chen, A.A.; Thomas, D.K.; Ong, L.L.; Schwartz, R.E.; Golub, T.R.; Bhatia, S.N. Humanized mice with ectopic artificial liver tissues. Proc. Natl. Acad. Sci. USA 2011, 108, 11842–11847.

6. Dhawan, A.; Puppi, J.; Hughes, R.D.; Mitry, R.R. Human hepatocyte transplantation: Current experience and future challenges. Nat. Rev. Gastroenterol. Hepatol. 2010, 7, 288–298.

7. Fox, I.J.; Roy-Chowdhury, J. Hepatocyte transplantation. J. Hepatol. 2004, 40, 878–886.

8. Zhang, J.; Zhao, X.; Liang, L.; Li, J.; Demirci, U.; Wang, S. A decade of progress in liver regenerative medicine. Biomaterials 2018, 157, 161–176.

9. Huh, D.; Hamilton, G.A.; Ingber, D.E. From 3D cell culture to organs-on-chips. Trends. Cell Biol. 2011, 21, 745–754.

10. Bhatia, S.N.; Ingber, D.E. Microfluidic organs-on-chips. Nat. Biotechnol. 2014, 32, 760–772.

11. Rajendran, D.; Hussain, A.; Yip, D.; Parekh, A.; Shrirao, A.; Cho, C.H. Long-term liver-specific functions of hepatocytes in electrospun chitosan nanofiber scaffolds coated with fibronectin. J. Biomed. Mater. Resa. 2017, 105, 2119–2128.

12. Lee, H.; Chae, S.; Kim, J.Y.; Han, W.; Kim, J.; Choi, Y.; Cho, D.W. Cell-printed 3D liver-on-a-chip possessing a liver microenvironment and biliary system. Biofabrication. 2019, 11(2):025001. doi:10.1088/1758-5090/aaf9fa.

13. Stevens, K.R.; Miller, J.S.; Blakely, B.L.; Chen, C.S.; Bhatia, S.N. Degradable hydrogels derived from PEG-diacrylamide for hepatic tissue engineering. J. Biomed. Mater Resa. 2015, 103, 3331–3338.

14. Crapo, P.M.; Gilbert, T.W.; Badylak, S.F. An overview of tissue and whole organ decellularization processes. Biomaterials 2011, 32, 3233–3243.

15. Peloso, A.; Dhal, A.; Zambon, J.P.; Li, P.; Orlando, G.; Atala, A.; Soker, S. Current achievements and future perspectives in whole-organ bioengineering. Stem Cell Res. Ther. 2015, 6, 107, doi:10.1186/s13287-015-0089-y.

16. Mason, C.; Dunnill, P. A brief definition of regenerative medicine. Regen. Med. 2008, 3, 1–5.

17. Katari, R.; Peloso, A.; Orlando, G. Tissue engineering and regenerative medicine: Semantic considerations for an evolving paradigm. Front. Bioeng. Biotechnol. 2015, 2, 57, doi:10.3389/fbioe.2014.00057.

18. Thomas, L. Notes of a biology-watcher. The planning of science. N. Engl. J. Med. 1973, 289, 89–90.

19. Orlando, G.; Soker, S.; Stratta, R.J. Organ bioengineering and regeneration as the new Holy Grail for organ transplantation. Ann. Surg. 2013, 258, 221–232.

20. Bourlière, M.; Gordon, S.C.; Flamm, S.L.; Cooper, C.L.; Ramji, A.; Tong, M.; Ravendhran, N.; Vierling, J.M.; Tran, T.T.; Pianko, S. et al. POLARIS-1 and POLARIS-4 Investigators. Sofosbuvir, Velpatasvir, and Voxilaprevir for Previously Treated HCV Infection. N. Engl. J. Med. 2017, 376, 2134–2146.

21. Toso, C.; Pinto Marques, H.; Andres, A.; Castro Sousa, F.; Adam, R.; Kalil, A.; Clavien, P.A.; Furtado, E.; Barroso, E.; Bismuth, H. Compagnons Hépato-Biliaires Group. Liver transplantation for colorectal liver metastasis: Survival without recurrence can be achieved. Liver Transpl. 2017, 23, 1073–1076.

22. Peloso, A.; Katari, R.; Zambon, J.P.; Orlando, G. Sisyphus, the Giffen's paradox and the Holy Grail: Time for organ transplantation to transition toward a regenerative medicine-focused type of research. Expert Rev. Clin. Immunol. 2013, 9, 883–885.

23. Ott, H.C.; Matthiesen, T.S.; Goh, S.K.; Black, L.D.; Kren, S.M.; Netoff, T.I.; Taylor, D.A. Perfusion-decellularized matrix: Using nature's platform to engineer a bioartificial heart. Nat. Med. 2008, 14, 213–221.

24. Haycock, J.W. 3D Cell Culture: A Review of Current Approaches and Techniques. Methods Mol. Biol. 2011, 695, 1–15.

25. Langer, R.; Tirrell, D.A. Designing materials for biology and medicine. Nature 2004, 428, 487–492.

26. Lv, D.; Hu, Z.; Lu, L.; Lu, H.; Xu, X. Three-dimensional cell culture: A powerful tool in tumor research and drug discovery. Oncol. Lett. 2017, 14, 6999–7010.

27. Hench, L.L.; Jones, J.R. Biomaterials artificial organs and tissue engineering. 1st Edition; Woodhead Publishing: Cambridge, UK, 2005.

28. Kizawa, H.; Nagao, E.; Shimamura, M.; Zhang, G.; Torii, H. Scaffold-free 3D bio-printed human liver tissue stably maintains metabolic functions useful for drug discovery. Biochem. Biophys. Rep. 2017, 10, 186–191.

29. Luo, Y.; Lou, C.; Zhang, S.; Zhu, Z.; Xing, Q.; Wang, P.; Liu, T.; Liu, H.; Li, C.; Shi, W. et al. Three-dimensional hydrogel culture conditions promote the differentiation of human induced pluripotent stem cells into hepatocytes. Cytotherapy 2018, 20, 95–107.

30. Tapias, L.F.; Ott, H.C. Decellularized scaffolds as a platform for bioengineered organs. Curr. Opin. Organ Transplant. 2014, 19, 145–152.

31. Petrosyan, A.; Orlando, G.; Peloso, A.; Wang, Z.; Farney, A.C.; Rogers, G.; Katari, R.; Da Sacco, S.; Sedrakyan, S.; De Filippo, R.E. et al. Understanding the bioactivity of stem cells seeded on extracellular matrix scaffolds produced from discarded human kidneys: A critical step towards a new generation bio-artificial kidney. CellR4 2015, 3, e1401.

32. Verstegen, M.M.A.; Willemse, J.; van den Hoek, S.; Kremers, G.J.; Luider, T.M.; van Huizen, N.A.; Willemssen, F.E.J.A.; Metselaar, H.J.; IJzermans, J.N.M.; van der Laan, L.J.W. et al. Decellularization of Whole Human Liver Grafts Using Controlled Perfusion for Transplantable Organ Bioscaffolds. Stem Cells Dev. 2017, 26, 1304–1315.

33. Grant, R.; Hay, D.; Callanan, A. From scaffold to structure: The synthetic production of cell derived extracellular matrix for liver tissue engineering. Biomed. Phys. Eng. Express 2018, 4, doi:10.1088/2057-1976/aacbe1

34. Török, E.; Lutgehetmann, M.; Bierwolf, J.; Melbeck, S.; Düllmann, J.; Nashan, B.; Ma, P.X.; Pollok, J.M. Primary human hepatocytes on biodegradable poly(l-lactic acid) matrices: A promising model for improving transplantation efficiency with tissue engineering. Liver Transplant. 2011, 17, 104–114.

35. Grant, R.; Hay, D.C.; A. Callanan, A. Drug-Induced Hybrid Electrospun Poly-Capro-Lactone: Cell-Derived Extracellular Matrix Scaffold for Liver Tissue Engineering. Tissue Eng. Part A. 2017, 23, 650–662.

36. Linti, C.; Zipfel, A.; Schenk, M.; Dauner, M.; Doser, M.; Viebahn, R.; Becker, H.D.; Planck, H. Cultivation of porcine hepatocytes in polyurethane nonwovens as part of a biohybrid liver support system, Int. J. Artif. Organs. 2002, 25, 994–1000.

37. Agarwal, T.; Narayan, R.; Maji, S.; Ghosh, S.K.; Maiti, T.K. Decellularized caprine liver extracellular matrix as a 2D substrate coating and 3D hydrogel platform for vascularized liver tissue engineering. J. Tissue Eng. Regen. Med., 2018, 12, e1678–e1690, doi:10.1002/term.2594.

38. Fasolino, I.; Guarino, V.; Guarino, V.; Marrese, M.; Cirillo, V.; Vallifuoco, M.; Tamma, M.L.; Vassallo, V.; Bracco, A.; Calise, F. et al. HepG2 and human healthy hepatocyte in vitro culture and co-culture in PCL electrospun platforms. Biomed. Mater. 2018, 13(1):015017, doi:10.1088/1748-605X/aa8c51.

39. Lee, J.W.; Choi, Y.J.; Yong, W.J.; Pati, F.; Shim, J.H.; Kang, K.S.; Kang, I.H.; Park, J.; Cho, D.W. Development of a 3D cell printed construct considering angiogenesis for liver tissue engineering. Biofabrication 2016, 8(1):015007, doi:10.1088/1758-5090/8/1/015007.

40. Gaffey, A.C.; Chen, M.H.; Venkataraman, C.M.; Trubelja, A.; Rodell, C.B.; Dinh, P.V.; Hung, G.; MacArthur, J.W.; Soopan, R.V.; Burdick, J.A. et al. Injectable shear-thinning hydrogels used to deliver endothelial progenitor cells, enhance cell engraftment, and improve ischemic myocardium. J. Thorac. Cardiovasc. Surg. 2015, 150, 1268–1276.

41. Ghaedi, M.; Soleimani, M.; Shabani, I.; Duan, Y.; Lotfi, A.S. Hepatic differentiation from human mesenchymal stem cells on a novel nanofiber scaffold. Cell Mol. Biol. Lett. 2012, 17, 89–106.

42. Faulk, D.M.; Carruthers; C.A.; Warnerm, H.J.; Kramer, C.R.; Reing, J.E.; Zhang, L.; D'Amore, A.; Badylak, SF. The effect of detergents on the basement membrane complex of a biologic scaffold material. Acta Biomater. 2014, 10, 183–193.

43. Lin, X. Z. et al. Computer morphometry for quantitative measurement of liver fibrosis: Comparison with Knodell's score, colorimetry and conventional description reports. J. Gastroenterol. Hepatol. (1998). doi:10.1111/j.1440-1746.1998.tb00549.x)

44. Bedossa, P. & Paradis, V. Liver extracellular matrix in health and disease. Journal of Pathology (2003). doi:10.1002/path.1397).

45. Evans, D.W.; Moran, E.C.; Baptista, P.M.; Soker, S.; Sparks, J.L. Scale-dependent mechanical properties of native and decellularized liver tissue. Biomech. Model. Mechanobiol. 2013, 12, 569–580.

46. Moran, E.C.; Baptista, P.M.; Evans, D.W.; Soker, S.; Sparks, J.L. Evaluation of parenchymal fluid pressure in native and decellularized liver tissue. Biomed. Sci. Instrum. 2012, 48, 303–309.

47. Sánchez-Romero, N.; Sainz-Arnal, P.; Pla-Palacín, I.; Dachary, P.R.; Almeida, H.; Pastor, C.; Soto, D.R.; Rodriguez, M.C.; Arbizu, E.O.; Martinez, L.B. et al. The role of extracellular matrix on liver stem cell fate: A dynamic relationship in health and disease. Differentiation 2019, 106, 49–56.

48. Uygun, B.E.; Soto-Gutierrez, A.; Yagi, H.; Izamis, M.L.; Guzzardi, M.A.; Shulman, C.; Milwid, J.; Kobayashi, N.; Tilles, A.; Berthiaume, F. et al. Organ reengineering through development of a transplantable recellularized liver graft using decellularized liver matrix. Nat. Med. 2010, 16, 814–820.

49. Jaramillo, M.; Yeh, M.H.; Yarmush, M.L.; Uygun, B.E. Decellularized human liver extracellular matrix (hDLM)-mediated hepatic differentiation of human induced pluripotent stem cells (hIPSCs). J. Tissue Eng. Regen. Med. 2018, 12, e1962–e1973, doi: 10.1002/term.2627.

50. Arenas-Herrera, J.E.; Ko, I.K.; Atala, A.; Yoo, J.J. Decellularization for whole organ bioengineering. Biomed. Mater. 2013, 8(1), doi:10.1088/1748-6041/8/1/014106.

51. Keane, T. J., Swinehart, I. T. & Badylak, S. F. Methods of tissue decellularization used for preparation of biologic scaffolds and in vivo relevance. Methods (2015).doi:10.1016/j.ymeth.2015.03.005

52. Grauss, R. W. et al. Histological evaluation of decellularised porcine aortic valves: Matrix changes due to different decellularisation methods. in European Journal of Cardio-thoracic Surgery (2005). doi:10.1016/j.ejcts.2004.12.052

53. Lee RC. Cell injury by electric forces. Ann N Y Acad Sci. 2005; 1066:85–91. [PubMed:16533920]

54. Crapo PM, Gilbert TW, Badylak SF. An overview of tissue and whole organ decellularization processes. Biomaterials. 2011 Apr;32(12):3233-43. doi:10.1016/j.biomaterials.2011.01.057.

55. Dong, X. et al. RGD-modified acellular bovine pericardium as a bioprosthetic scaffold for tissue engineering. J. Mater. Sci. Mater. Med. (2009).doi:10.1007/s10856-009-3791-4

56. Reing, J. E. et al. The effects of processing methods upon mechanical and biologic properties of porcine dermal extracellular matrix scaffolds. Biomaterials (2010). doi:10.1016/j.biomaterials.2010.07.083

57. Xu CC, Chan RW, Tirunagari N. A biodegradable, acellular xenogeneic scaffold for regeneration of the vocal fold lamina propria. Tissue Eng. 2007; 13(3):551–566. [PubMed: 17518602]

58. 58 tam Arnold, T. & Linke, D. The use of detergents to purify membrane proteins. Curr.Protoc. protein Sci. / Editor. board, John E Coligan [et al] (2008).

59. Peloso, A. et al. Abdominal organ bioengineering: Current status and future perspectives. Minerva Chir. (2015).

60. Meyer SR, Chiu B, Churchill TA, Zhu L, Lakey JR, Ross DB. Comparison of aortic valve allograft decellularization techniques in the rat. J Biomed Mater Res A. 2006; 79(2):254–262. [PubMed:16817222]

61. Petersen TH, Calle EA, Zhao L, Lee EJ, Gui L, Raredon MB, et al. Tissue-engineered lungs for in vivo implantation. Science. 2010; 329(5991):538–541. [PubMed: 20576850]

62. Grauss RW, Hazekamp MG, Oppenhuizen F, van Munsteren CJ, Gittenberger-de Groot AC,DeRuiter MC. Histological evaluation of decellularised porcine aortic valves: matrix changes due to different decellularisation methods. Eur J Cardiothorac Surg. 2005; 27(4):566–571. [PubMed:15784352]

63. Yang B, Zhang Y, Zhou L, Sun Z, Zheng J, Chen Y, et al. Development of a porcine bladder acellular matrix with well-preserved extracellular bioactive factors for tissue

engineering. Tissue Eng Part C Methods. 2010; 16(5):1201–1211. [PubMed: 20170425

64. Hassanein, W.; Uluer, M.C.; Langford, J.; Woodall, J.D.; Cimeno, A.; Dhru, U.; Werdesheim, A.; Harrison, J.; Rivera-Pratt, C.; Klepfer, S.; et al. Recellularization via the bile duct supports functional allogenic and xenogenic cell growth on a decellularized rat liver scaffold. Organogenesis 2017, 13, 16–27.

65. Pla-Palacín, I.; Sainz-Arnal, P.; Morini, S.; Almeida, M.; Baptista, P.M. Liver bioengineering using decellularized whole-liver scaffolds. Methods Mol Biol. 2018, 1577, 293–305.

66. Mazza, G.; Rombouts, K.; Rennie Hall, A.; Urbani, L.; Vinh Luong, T.; Al-Akkad, W.; Longato, L.; Brown, D.; Maghsoudlou, P.; Dhillon, A.P. et al. Decellularized human liver as a natural 3D-scaffold for liver bioengineering and transplantation. Sci. Rep. 2015, 5, 13079, doi:10.1038/srep13079.

67. Wang, Y.; Cui, C.B.; Yamauchi, M.; Miguez, P.; Roach, M.; Malavarca, R.; Costello, M.J.; Cardinale, V.; Wauthier, E.; Barbier, C. et al. Lineage restriction of human hepatic stem cells to mature fates is made efficient by tissue-specific biomatrix scaffolds. Hepatology 2011, 53, 293–305.

68. Bao, J.; Shi, Y.; Sun, H.; Yin, X.; Yang, R.; Li, L.; Chen, X.; Bu, H. Construction of a portal implantable functional tissue-engineered liver using perfusion-decellularized matrix and hepatocytes in rats. Cell Transplant. 2011, 20, 753–766.

69. Soto-Gutierrez, A.; Zhang, L.; Medberry, C.; Fukumitsu, K.; Faulk, D.; Jiang, H.; Reing, J.; Gramignoli, R.; Komori, J.; Ross, M. et al. A Whole-Organ Regenerative Medicine Approach for Liver Replacement. Tissue Eng. Part C. Methods. 2011, 17, 677–686.

70. Baptista, P.M.; Siddiqui, M.M.; Lozier, G.; Rodriguez, S.R.; Atala, A.; Soker, S. The use of whole organ decellularization for the generation of a vascularized liver organoid. Hepatology 2011, 53, 604–617.

71. Lang, R.; Stern, M.M.; Smith, L.; Liu, Y.; Bharadwaj, S.; Liu, G.; Baptista, P.M.; Bergman, C.R.; Soker, S.; Yoo, J.J. et al Three-dimensional culture of hepatocytes on porcine liver tissue-derived extracellular matrix. Biomaterials 2011, 32, 7042–7052.

72. Barakat. O.; Abbasi; S.; Rodriguez, G.; Rios, J.; Wood, R.P.; Ozaki, C.; Holley, L.S.; Gauthier, P.K. Use of decellularized porcine liver for engineering humanized liver organ. J. Surg. Res. 2012, 173(1), e11–e25, doi:10.1016/j.jss.2011.09.033.

73. Wang, X.; Cui, J.; Zhang, B.Q.; Zhang, H.; Bi, Y.; Kang, Q.; Wang, N.; Bie, P.; Yang, Z.; Wang, H. et al. Decellularized liver scaffolds effectively support the proliferation and differentiation of mouse fetal hepatic progenitors. J. Biomed. Mater. Res. A. 2014, 102, 1017–1025

74. Yagi, H.; Fukumitsu, K.; Fukuda, K.; Kitago, M.; Shinoda, M.; Obara, H.; Itano, O.; Kawachi, S.; Tanabe, M.; Coudriet, G.M. et al. Human-scale whole-organ bioengineering for liver transplantation: A regenerative medicine approach. Cell Transplant. 2013, 22, 231–242.

75. Kadota, Y.; Yagi, H.; Inomata, K.; Matsubara, K.; Hibi, T.; Abe, Y.; Kitago, M.; Shinoda, M.; Obara, H.; Itano, O. et al. Mesenchymal stem cells support hepatocyte function in engineered liver grafts. Organogenesis 2014, 10, 268–277.

76. Jiang, W.C.; Cheng, Y.H.; Yen, M.H.; Chang, Y.; Yang, V.W.; Lee, O.K. Cryo-chemical decellularization of the whole liver for mesenchymal stem cells-based functional hepatic tissue engineering. Biomaterials 2014, 35, 3607–3617.

77. Navarro-Tableros, V.; Herrera Sanchez, M.B.; Figliolini, F.; Romagnoli, R.; Tetta, C.; Camussi, G. Recellularization of Rat Liver Scaffolds by Human Liver Stem Cells. Tissue Eng. Parta. 2015, 21, 1929–1939.

78. Ko, I.K.; Peng, L.; Peloso, A.; Smith, C.J.; Dhal, A.; Deegan, D.B.; Zimmerman, C.; Clouse, C.; Zhao, W.; Shupe, T.D. et al. Bioengineered transplantable porcine livers with re-endothelialized vasculature. Biomaterials 2015, 40, 72–79.

79. Bruinsma, B.G.; Kim, Y.; Berendsen, T.A.; Ozer, S.; Yarmush, M.L.; Uygun, B.E. Layer-by-layer heparinization of decellularized liver matrices to reduce thrombogenicity of tissue engineered grafts. J. Clin. Transl. Res. 2015, 1, 48–56.

80. Wang, B.; Jakus, A.E.; Baptista, P.M.; Soker, S.; Soto-Gutierrez, A.; Abecassis, M.M.; Shah, R.N.; Wertheim, J.A. Functional Maturation of Induced Pluripotent Stem Cell Hepatocytes in Extracellular Matrix-A Comparative Analysis of Bioartificial Liver Microenvironments. Stem Cells Transl. Med. 2016, 5, 1257–1267.

81. Zhou, P.; Huang, Y.; Guo, Y.; Wang, L.; Ling, C.; Guo, Q.; Wang, Y.; Zhu, S.; Fan, X.; Zhu, M. et al Decellularization and Recellularization of Rat Livers With Hepatocytes and Endothelial Progenitor Cells. Artif. Organs. 2016, 40, E25–E38, doi:10.1111/aor.12645.

82. Park, K.M.; Hussein, K.H.; Hong, S.H.; Ahn, C.; Yang, S.R.; Park, S.M.; Kweon, O.K.; Kim, B.M.; Woo, H.M. Decellularized Liver Extracellular Matrix as Promising Tools for Transplantable Bioengineered Liver Promotes Hepatic Lineage Commitments of Induced Pluripotent Stem Cells. Tissue Eng. Part A. 2016, 22, 449–460.

83. Hussein, K.H.; Park, K.M.; Kang, K.S.; Woo, H.M. Heparin-gelatin mixture improves vascular reconstruction efficiency and hepatic function in bioengineered livers. Acta Biomater. 2016, 1, 82–93.

84. Ogiso, S.; Yasuchika, K.; Fukumitsu, K.; Ishii, T.; Kojima, H.; Miyauchi, Y.; Yamaoka, R.; Komori, J.; Katayama, H.; Kawai, T. et al Efficient recellularisation of decellularised whole-liver grafts using biliary tree and foetal hepatocytes. Sci. Rep. 2016, 6, 35887, doi:10.1038/srep35887.

85. Wen, X.; Huan, H.; Wang, X.; Chen, X.; Wu, L.; Zhang, Y.; Liu, W.; Bie, P.; Xia, F. Sympathetic neurotransmitters promote the process of recellularization in decellularized liver matrix via activating the IL-6/Stat3 pathway. Biomed. Mater. 2016, 11(6), 065007, doi:10.1088/1748-6041/11/6/065007.

86. Lorvellec, M.; Scottoni, F.; Crowley, C.; Fiadeiro, R.; Maghsoudlou, P.; Pellegata, A.F.; Mazzacuva, F.; Gjinovci, A.; Lyne, A.M.; Zulini, J. et al. Mouse decellularised liver scaffold improves human embryonic and induced pluripotent stem cells differentiation into hepatocyte-like cells. PLoS ONE, 2017, 12, e0189586, doi:10.1371/journal.pone.0189586.

87. Mazza, G.; Al-Akkad, W.; Telese, A.; Longato, L.; Urbani, L.; Robinson, B.; Hall, A.; Kong, K.; Frenguelli, L.; Marrone, G. et al. Rapid production of human liver scaffolds for functional tissue engineering by high shear stress oscillation-decellularization. Sci. Rep. 2017, 7(1), 5534, 10.1038/s41598-017-05134-1.

88. Shupe, T.; Williams, M.; Brown, A.; Willenberg, B.; Petersen, B. E. Method for the decellularization of intact rat liver. Organogenesis 2010, 6, 134–136.

89. Yang, W.; Xia, R.; Zhang, Y.; Zhang, H.; Bai, L. Decellularized liver scaffold for liver regeneration. Methods Mol. Biol. 2018, 1577, 11–23.

90. Struecker, B.; Butter, A.; Hillebrandt, K.; Polenz, D.; Reutzel-Selke, A.; Tang, P.; Lippert, S.; Leder, A.; Rohn, S.; Geisel, D. et al. Improved rat liver decellularization by arterial perfusion under oscillating pressure conditions. J. Tissue Eng. Regen. Med. 2017, 11, 531–541.

91. Ren, H.; Shi, X.; Tao, L.; Xiao, J.; Han, B.; Zhang, Y.; Yuan, X.; Ding, Y. Evaluation of two decellularization methods in the development of a whole-organ decellularized rat liver scaffold. Liver Int. 2013, 33, 448–458.

92. Mazza, G.; Al-Akkad, W.; Rombouts, K.; Pinzani, M. Liver tissue engineering: From implantable tissue to whole organ engineering. Hepatol. Commun. 2018, 2, 131–141.

93. Mirmalek-Sani, S.H.; Sullivan, D.C.; Zimmerman, C.; Shupe, T.D.; Petersen, B. E. Immunogenicity of decellularized porcine liver for bioengineered hepatic tissue. Am. J. Pathol. 2013, 183, 558–565.

94. Yagi, H.; Fukumitsu, K.; Fukuda, K.; Kitago, M.; Shinoda, M.; Obara, H.; Itano, O.; Kawachi, S.; Tanabe, M.; Coudriet, G.M. et al. Human-scale whole-organ bioengineering for liver transplantation: A regenerative medicine approach. Cell Transplant. 2013, 22, 231–242.

95. Struecker, B.; Hillebrandt, K.H.; Voitl, R.; Butter, A.; Schmuck, R.B.; Reutzel-Selke, A.; Geisel, D.; Joehrens, K.; Pickerodt, P.A.; Raschzok, N. et al. Porcine Liver Decellularization Under Oscillating Pressure Conditions: A Technical Refinement to

Improve the Homogeneity of the Decellularization Process. Tissue Eng. Part C. Methods 2014, 21, 303–313.

96. Gao, M.; Wang, Y.; He, Y.; Li, Y.; Wu, Q.; Yang, G.; Zhou, Y.; Wu, D.; Bao, J.; Bu, H. Comparative evaluation of decellularized porcine liver matrices crosslinked with different chemical and natural crosslinking agents. Xenotransplantation 2019, 26(1), e12470, doi:10.1111/xen.12470.

97. Y. Wang et al., "Genipin crosslinking reduced the immunogenicity of xenogeneic decellularized porcine whole-liver matrices through regulation of immune cell proliferation and polarization.," Sci. Rep., vol. 6, p. 24779, Apr. 2016.

98. Bao, J.; Wu, Q.; Sun, J.; Zhou, Y.; Wang, Y.; Jiang, X.; Li, L.; Shi, Y.; Bu, H. Hemocompatibility improvement of perfusion-decellularized clinical-scale liver scaffold through heparin immobilization. Sci. Rep. 2015, 5, 10756, doi:10.1038/srep10756.

99. Reflection paper on classification of advanced therapy medicinal products. 13 April 2012 EMA/CAT/600280/2010 Committee for Advanced Therapies.

100. Zhou, P.; Lessa, N.; Estrada, D.C.; Severson, E.B.; Lingala, S.; Zern, M.A.; Nolta, J.A.; Wu, J. Decellularized liver matrix as a carrier for the transplantation of human fetal and primary hepatocytes in mice. Liver Transplant. 2011, 17, 418–427.

101. Kmieć, Z.; Cooperation of Liver Cells in Health and Disease. Adv. Anat. Embryol. Cell Biol. 2001, 161, 1–151.

102. Mao, S.A.; Glorioso, J.M.; Nyberg, S.L. Liver regeneration. Translational Research: The Journal of Laboratory and Clinical Medicine. Transl. Res. 2014, 163, 352–362.

103. Yuan, J.; Liu, L.; Shimada, M.; Wang, A.; Ruhnke, M.; Heeckt, P.; Muller, A.R.; Nussler, N.C.; Neuhaus, P.; Nussler, A. Induction, expression and maintenance of cytochrome P450 isoforms in long-term cultures of primary human hepatocytes. ALTEX, 2004, 21, 3–11.

104. Gupta, S.; Gorla, G.R.; Irani, A.N. Hepatocyte transplantation: Emerging insights into mechanisms of liver repopulation and their relevance to potential therapies. J. Hepatol. 1999, 30, 162–70.

105. Niwa, H. Mechanisms of Stem Cell Self-Renewal. In Essentials of Stem Cell Biology, Third Edition; Academic Press: London, UK 2013; Volume 7, 81–94.

106. Banas, A.; Yamamoto, Y.; Teratani, T.; Ochiya T. Stem cell plasticity: Learning from hepatogenic differentiation strategies. Dev. Dynamics. 2007, 236, 3228–3241.

107. Takayama, K.; Nagamoto, Y.; Nagamoto, Y.; Kishimoto, K.; Tashiro, K.; Sakurai, F.; Tachibana, M.; Kanda, K.; Hayakawa, T.; Furue, M.K. et al. 3D spheroid culture of hESC/hiPSC-derived hepatocyte-like cells for drug toxicity testing. Biomaterials 2013, 34, 1781–1789.

108. Ramasamy, T.S.; Yu, J.S.L.; Selden, C.; Hodgson, H.; Cui, W. Application of Three-Dimensional Culture Conditions to Human Embryonic Stem Cell-Derived Definitive Endoderm Cells Enhances Hepatocyte Differentiation and Functionality. Tissue Eng. Part A. 2013, 19, 360–367.

109. K. Subramanian; Raju, R.; Firpo, M.; O'Brien, T.D.; Verfaillie, C.M.; Hu, W.S. Spheroid Culture for Enhanced Differentiation of Human Embryonic Stem Cells to Hepatocyte-Like Cells. Stem Cells Dev. 2014, 23, 124–131.

110. Sancho-Bru, P.; Najimi, M.; Caruso, M.; Pauwelyn, K.; Cantz, T.; Forbes, S.; Roskams, T.; Ott, M.; Gehling, U.; Sokal, E. et al. Stem and progenitor cells for liver repopuletion: Can we standardise the process from bench to bedside? Gut 2009, 58, 594–603.

111. Thomson, J.A.; Itskovitz-Eldor, J.; Shapiro, S.S.; Waknitz, M.A.; Swiergiel, J.J.; Marshall, V.S.; Jones, J.M. Embryonic stem cell lines derived from human blastocysts. Science 1998, 282, 1145–1147.

112. Teramoto, K.; Asahina, K.; Kumashiro, Y.; Kakinuma, S.; Chinzei, R.; Shimizu-Saito, K.; Tanaka, Y.; Teraoka, H.; Arii, S. Hepatocyte differentiation from embryonic stem

cells and umbilical cord blood cells. J. Hepato-Biliary-Pancreat. Surg. 2005, 12, 196–202.

113. Wang, Y.; Zhang, Y.; Zhang, S.; Peng, G.; Liu, T.; Li, Y.; Xiang, D.; Wassler, M.J.; Shelat, H.S.; Geng, Y. Rotating Microgravity-Bioreactor Cultivation Enhances the Hepatic Differentiation of Mouse Embryonic Stem Cells on Biodegradable Polymer Scaffolds. Tissue Eng. Part A 2012, 18, 2376–2385.

114. Zhang, W.; Li, W.; Liu, B.; Wang, P.; Li, W.; Zhang H. Efficient generation of functional hepatocyte-like cells from human fetal hepatic progenitor cells in vitro. J. Cell. Physiol. 2012, 227, 2051–2058.

115. Lees, J.G.; Lim, S.A.; Croll, T.; Williams, G.; Lui, S.; Cooper-White, J.; McQuade, L.R.; Mathiyalagan, B.; Tuch, B.E. Transplantation of 3D scaffolds seeded with human embryonic stem cells: Biological features of surrogate tissue and teratoma-forming potential. Regen. Med. 2007, 2, 289–300.

116. Vestentoft, P.S. Development and molecular composition of the hepatic progenitor cell niche. Dan. Med J. 2013, 60, B4640.

117. Khun, D.N.; Scheers, I.; Ehnert, S.; Jazouli, N.; Nyabi, O.; Buc-Calderon, P.; Meulemans, A.; Nussler, A.; Sokal, E.; Najimi, M. In vitro Differentiated adult human liver progenitor cells display mature hepatic metabolic functions: A potential tool for in vitro pharmacotoxicological testing. Cell Transplant. 2011, 20, 287–302.

118. Strick-Marchand, H.; Weiss, M.C. Inducible differentiation and morphogenesis of bipotential liver cell lines from wild-type mouse embryos. Hepatology 2002, 36, 794–804.

119. O'Donoghue, K.; Fisk, N.M. Fetal stem cells. Best Pr. Res. Clin. Obs. Gynaecol. 2004, 18, 853–875.

120. Zhang, W.; Li, W.; Liu, B.; Wang, P.; Li, W.; Zhang H. Efficient generation of functional hepatocyte-like cells from human fetal hepatic progenitor cells in vitro. J. Cell. Physiol. 2012, 227, 2051–2058.

121. Satija, N.K.; Singh, VK.; Verma, Y.K.; Gupta, P.; Sharma, S.; Afrin, F.; Sharma, M.; Sharma, P.; Tripathi, R.P.; Gurudutta, G.U. Mesenchymal stem cell-based therapy: A new paradigm in regenerative medicine. J. Cell. Mol. Med. 2009, 13, 4385–4402.

122. Ji, R.; Zhang, N.; You, N.; Li, Q.; Liu, W.; Jiang, N.; Liu, J.; Zhang, H.; Wang, D.; Tao, K. et al. The differentiation of MSCs into functional hepatocyte-like cells in a liver biomatrix scaffold and their transplantation into liver-fibrotic mice. Biomaterials 2012, 33, 8995–9008.

123. Li, J.; Tao, R.; Wu, W.; Cao, H.; Xin, J.; Li, J.; Guo, J.; Jiang, L.; Gao, C.; Demetriou, A.A. 3D PLGA Scaffolds Improve Differentiation and Function of Bone Marrow Mesenchymal Stem Cell–Derived Hepatocytes. Stem Cells Dev. 2010, 19, 1427–1436.

124. Christ, B.; Dollinger, M.M. The generation of hepatocytes from mesenchymal stem cells and engraftment into the liver. Curr. Opin. Organ Transplant. 2011, 16, 69–75.

125. Li, Y.; Wu, Q.; Wang, Y.; Li, L.; Chen, F.; Shi, Y.; Bao, J.; Bu, H. Construction of bioengineered hepatic tissue derived from human umbilical cord mesenchymal stem cells via aggregation culture in porcine decellularized liver scaffolds. Xenotransplantation 2017, 24(1), e12258, doi:10.1111/xen.12285.

126. Okita, K.; Ichisaka, T.; Yamanaka, S. Generation of germline-competent induced pluripotent stem cells. Nature 2007, 19, 313–317.

127. Jia, F.; Wilson, K.D.; Sun, N.; Gupta, D.M.; Huang, M.; Li, Z.; Panetta, N.J.; Chen, Z.Y.; Robbins, R.C.; Kay, M.A.; et al. A nonviral minicircle vector for deriving human iPS cells. Nat. Methods 2010, 7, 197–199.

128. Subba Rao, M.; Sasikala, M.; Reddy, D. N. Thinking outside the liver: Induced pluripotent stem cells for hepatic applications. World J. Gastroenterol. 2013, 19, 3385–3396.

129. Takebe, T.; Sekine, K.; Enomura, M.; Koike, H.; Kimura, M.; Ogaeri, T.; Zhang, R.R.; Ueno, Y.; Zheng, Y.W.; Koike, N. et al. Vascularized and functional human liver from an iPSC-derived organ bud transplant. Nature 2013, 499, 481–484.

130. Yamanaka, S.; Blau, H.M. Nuclear reprogramming to a pluripotent state by three approaches. Nature 2010, 465, 704–712.

131. Shi, Y.; Inoue, H.; Wu, J.C.; Yamanaka, S. Induced pluripotent stem cell technology: A decade of progress. Nat. Rev. Drug Discov. 2017, 16, 115–130.

132. Soto-Gutierrez, A.; Tafaleng, E.; Kelly, V.; Roy-Chowdhury, J.; Fox I.J. Modeling and therapy of human liver diseases using induced pluripotent stem cells: How far have we come? Hepatology. 2011, 53, 708–711.

133. Kehtari, M.; Beiki, B.; Zeynali, B.; Hosseini, F.S.; Soleimanifar, F.; Kaabi, M.; Soleimani, M.; Enderami, S.E.; Kabiri, M.; Mahboudi, H. Decellularized Wharton's jelly extracellular matrix as a promising scaffold for promoting hepatic differentiation of human induced pluripotent stem cells. J. Cell Biochem. 2019, 120, 6683–6697.

134. Fitzpatrick, E.; Mitry, R.R.; Dhawan A. Human hepatocyte transplantation: State of the art. J. Intern. Med. 2009, 266, 339–357.

135. Martin, I.; Wendt, D.; Heberer M. The role of bioreactors in tissue engineering. Trends Biotechnol. 2004, 22, 80–86.

136. Wang, S.; Qu, X.; Zhao, R.C. Clinical applications of mesenchymal stem cells. J. Hematol. Oncol. 2012, 5, 19, doi:10.1186/1756-8722-5-19.

137. Tarassoli, S.P.; Jessop, Z.M.; Al-Sabah, A.; Gao, N.; Whitaker, S.; Doak, S.; Whitaker, I.S. Skin tissue engineering using 3D bioprinting: An evolving research field. J Plast. Reconstr. Aesthet. Surg. 2018, 71, 615–623.

138. Algzlan, H.; Varada, S. Three-Dimensional Printing of the Skin. JAMA Dermatol. 2015, 151(2), 207, doi:10.1001/jamadermatol.2014.1198.

139. Owens, C.M.; Marga, F.; Forgacs, G.; Heesch, C.M. Biofabrication and testing of a fully cellular nerve graft. Biofabrication. 2013, 5(4):045007. doi:10.1088/1758-5082/5/4/045007.

140. Alonzo, M.; AnilKumar, S.; Roman, B.; Tasnim, N.; Joddar, B. 3D Bioprinting of cardiac tissue and cardiac stem cell therapy Transl. Res. 2019, 211, 64–83.

141. Datta, P.; Ayan, B.; Ozbolat, I.T. Bioprinting for vascular and vascularized tissue biofabrication. Acta Biomater. 2017, 51, 1–20.

142. Datta, P.; Ozbolat, V.; Ayan, B.; Dhawan, A.; Ozbolat, I.T. Bone tissue bioprinting for craniofacial reconstruction. Biotechnol. Bioeng. 2017, 114, 2424–2431.

143. Kabirian, F.; Mozafari, M. Decellularized ECM-derived bioinks: Prospects for the future. Methods 2019, in press, doi:10.1016/j.ymeth.2019.04.019.

144. Choudhury, D.; Tun, H.W.; Wang, T.; Naing, M.W. Organ-Derived Decellularized Extracellular Matrix: A Game Changer for Bioink Manufacturing? Trends Biotechnol. 2018, 36, 787–805.

145. Lee, H.; Han, W.; Kim, H.; Ha, D.H.; Jang, J.; Kim, B.S.; Cho, D.W. Development of Liver Decellularized Extracellular Matrix Bioink for Three-Dimensional Cell Printing-Based Liver Tissue Engineering. Biomacromolecules 2017, 10, 1229–1237.

146. Jang, J.; Kim, T.G.; Kim, B.S.; Kim, S.W.; Kwon, S.M.; Cho, D.W. Tailoring mechanical properties of decellularized extracellular matrix bioink by vitamin B2-induced photo-crosslinking. Acta Biomater. 2016, 33, 88–95.

147. Clevers, H. Modeling Development and Disease with Organoids. Cell 2016, 165, 1586–159.

148. Huch, M.; Koo, B.K.; Modeling mouse and human development using organoid cultures. Development 2015, 142, 3113–3125.

149. Huch, M.; Gehart, H.; van Boxtel, R.; Hamer, K.; Blokzijl, F.; Verstegen, M.M.; Ellis, E.; van Wenum, M.; Fuchs, S.A.; de Ligt, J. et al. Long-term culture of genome-stable bipotent stem cells from adult human liver. Cell 2015, 15, 299–312.

150. Fang, Y.; Eglen, R.M. Three-Dimensional Cell Cultures in Drug Discovery and Development. SLAS Discov. 2017, 22, 456–472.

151. Hindley, C.J.; Cordero-Espinoza, L.; Huch, M. Organoids from adult liver and pancreas: Stem cell biology and biomedical utility. Dev. Biol. 2016, 15, 251–261.

152. Nantasanti, S.; de Bruin, Rothuizen, A.J.; Penning, L.C.; Schotanus, B.A. Concise Review: Organoids Are a Powerful Tool for the Study of Liver Disease and Personalized Treatment Design in Humans and Animals. Stem Cells Transl. Med. 2016, 5, 325–330.

153. Miyao, M.; Kotani, H.; Ishida, T.; Kawai, C.; Manabe, S.; Abiru, H.; Tamaki, K. Pivotal role of liver sinusoidal endothelial cells in NAFLD/NASH progression. Lab. Invest. 2015, 95, 1130–1144.

154. LeCluyse, E.L. Human hepatocyte culture systems for the in vitro evaluation of cytochrome P450 expression and regulation. Eur. J. Pharm. Sci. 2001,13, 343–368.

155. Mußbach, F.; Settmacher, U.; Dirsch, O.; Xie, C.; Dahmen, U. Bioengineered Livers: A New Tool for Drug Testing and a Promising Solution to Meet the Growing Demand for Donor Organs. Eur. Surg. Res. 2016, 57, 224–239.

156. Zhou, Q.; Li, L.; Li, J. Stem cells with decellularized liver scaffolds in liver regeneration and their potential clinical applications. Liver Int. 2015, 35, 687–694.

157. Natale, A.; Vanmol, K.; Arslan, A.; Van Vlierberghe, S.; Dubruel, P.; Van Erps, J.; Thienpont, H.; Buzgo, M.; Boeckmans, J.; De Kock, J. Technological advancements for the development of stem cell-based models for hepatotoxicity testing. Arch.Toxicol. 2019, 93, 1789–1805.

158. Vishwakarma, S.K.; Bardia, A.; Lakkireddy, C.R.; Nagarapu, R.; Habeeb, M.A.; and Khan, A.A.; Bioengineered humanized livers as better three-dimensional drug testing model system. World J. Hepatol. 2018, 27, 22–33

159. Roth, S. P. et al. Automated freeze-thaw cycles for decellularization of tendon tissue - a pilot study. BMC Biotechnol. 2017.

160. Stock P, Brückner S, Ebensing S, Hempel M, Dollinger MM, Christ B. The generation of hepatocytes from mesenchymal stem cells and engraftment into murine liver. Nat Protoc. 2010 Apr;5(4):617-27. doi: 10.1038/nprot.2010.7. Epub 2010 Mar 11. PubMed PMID: 20224562.

161. Al Ghrbawy NM, Afify RA, Dyaa N, El Sayed AA. Differentiation of Bone Marrow: Derived Mesenchymal Stem Cells into Hepatocyte-like Cells. Indian J Hematol Blood Transfus. 2016 Sep;32(3):276-83. doi: 10.1007/s12288-015-0581-7. Epub 2015 Aug 21. PubMed PMID: 27429519; PubMed Central PMCID: PMC4930759.

162. Lee KD, Kuo TK, Whang-Peng J et al. 2004; In vitro hepatic differentiation of human mesenchymal stem cells. Hepatology 40: 1275–1284.

163. Comite P, Cobianchi L, Avanzini MA, Zonta S, Mantelli M, Achille V, De Martino M, Cansolino L, Ferrari C, Alessiani M, Maccario R, Gandolfo GM, Dionigi P, Locatelli F, Bernardo ME. Isolation and ex vivo expansion of bone marrow-derived porcine mesenchymal stromal cells: potential for application in an experimental model of solid organ transplantation in large animals. Transplant Proc. 2010.

164. Dominici M, Le Blanc K, Mueller I, Slaper-Cortenbach I, Marini F, Krause D, Deans R, Keating A, Prockop Dj, Horwitz E. Minimal criteria for defining multipotent mesenchymal stromal cells. The International Society for Cellular Therapy position statement. Cytotherapy. 2006;8(4):315-7.